AD_____

Award Number: DAMD17-00-1-0040

TITLE: An Embryonic Growth Pathway is Reactivated in Human Prostate Cancer

PRINCIPAL INVESTIGATOR: Wade Bushman, M.D., Ph.D.

CONTRACTING ORGANIZATION: Northwestern University
Chicago, Illinois 60611-3008

REPORT DATE: February 2003

TYPE OF REPORT: Annual

PREPARED FOR: U.S. Army Medical Research and Materiel Command
Fort Detrick, Maryland 21702-5012

DISTRIBUTION STATEMENT: Approved for Public Release;
Distribution Unlimited

The views, opinions and/or findings contained in this report are those of the author(s) and should not be construed as an official Department of the Army position, policy or decision unless so designated by other documentation.

## Conclusions

The results of our study suggest that insurance status is a much bigger determinant of mammography receipt than managed care in an area. If anything, the propensity for managed care to reduce use of mammography is larger among insured women than among the uninsured. These results contradict those in a cross-sectional analysis where managed care is associated with greater mammography receipt. We believe that our results demonstrate the importance of controlling for unobserved characteristics across counties when estimating the effect of managed care penetration on health service use.

The results of our study suggest that the financial incentives created by managed care in a market do not lead to a reduction in service use. Furthermore, our results suggest that the reduction in the number of mammography providers found in earlier research does not threaten access to mammography, and managed care penetration is unlikely to explain declining mammography use among the uninsured in the 1990s.

## References


1. Baker LC. The effect of HMOs on fee-for-service health care expenditures: evidence from Medicare. J of Health Economics 1997;16:453-81.
2. Baker LC. Association of managed care market share and health expenditures for fee-for-service Medicare patients. JAMA 1999;281:432-37.
3. Baker LC, Brown ML. Managed care, consolidation among health care providers, and health care: evidence from mammography. RAND Journal of Economics 1999;30:351-74.
4. Rodgers J, Smith KE. Do Medicare HMOs reduce fee-for-service costs? Washington DC: Price Waterhouse LLP, Health Policy Economics Group; 1999.

# REPORT DOCUMENTATION PAGE

*Form Approved*
*OMB No. 074-0188*



| 1. AGENCY USE ONLY (Leave blank) | 2. REPORT DATE | 3. REPORT TYPE AND DATES COVERED |
|---|---|---|
| | February 2003 | Annual (15 Jan 00-14 Jan 03) |

**4. TITLE AND SUBTITLE**
An Embryonic Growth Pathway is Reactivated in Human Prostate Cancer

**5. FUNDING NUMBERS**
DAMD17-00-1-0040

**6. AUTHOR(S)**
Wade Bushman, M.D., Ph.D.

**7. PERFORMING ORGANIZATION NAME(S) AND ADDRESS(ES)**
Northwestern University
Chicago, Illinois 60611-3008

E-Mail: bushman@surgery.wisc.edu

**8. PERFORMING ORGANIZATION REPORT NUMBER**

**9. SPONSORING / MONITORING AGENCY NAME(S) AND ADDRESS(ES)**
U.S. Army Medical Research and Materiel Command
Fort Detrick, Maryland 21702-5012

**10. SPONSORING / MONITORING AGENCY REPORT NUMBER**

**11. SUPPLEMENTARY NOTES**

**12a. DISTRIBUTION / AVAILABILITY STATEMENT**
Approved for Public Release; Distribution Unlimited

**12b. DISTRIBUTION CODE**

**13. ABSTRACT (Maximum 200 Words)**

Epithelial-mesenchymal interactions in prostate cancer represent a promising target for drug therapies to arrest or slow tumor growth. For this potential to be realized, it is necessary to identify one specific epithelial-mesenchymal interaction which is critical for tumor growth. We have shown that *Sonic hedgehog* (*Shh*) signaling pathway is absolutely required for normal prostate development. Our preliminary studies show this pathway is expressed at very low levels in the normal adult prostate but reactivated in human prostate cancer. This research postulates that prostate cancer cells commandeer this normal epithelial-mesenchymal signaling pathway to recruit stromal cells to support abnormal tumor growth and tests the hypothesis that Shh signaling promotes prostate tumor growth. The primary goal of the study is to establish the concept that prostate tumor growth is promoted by re-activation of the Shh-Gli pathway and identify this as a novel target for drug treatment to slow or arrest prostate cancer growth.

**14. SUBJECT TERMS**
Prostate Cancer, Sonic Hedgehog

**15. NUMBER OF PAGES**
68

**16. PRICE CODE**

| 17. SECURITY CLASSIFICATION OF REPORT | 18. SECURITY CLASSIFICATION OF THIS PAGE | 19. SECURITY CLASSIFICATION OF ABSTRACT | 20. LIMITATION OF ABSTRACT |
|---|---|---|---|
| Unclassified | Unclassified | Unclassified | Unlimited |

## Table of Contents

**Introduction:**

This funded project addresses the role of hedgehog signaling in prostate cancer. Using a well characterized xenograft model, the purpose of the proposal is to characterize sonic hedgehog (Shh) expression in human prostate cancer, to examine the affect of Shh overexpression on prostate xenograft tumor growth, and to determine the effect of Shh loss of function on tumor growth.

**Body:**

The research goals in the statement of work have been addressed as planned. Specifically, the goals 1a, 1c, 2a, 2b, and 2d have been accomplished and those results are presented in the appended manuscript submitted for publication entitled, Shh Signaling, an Embryonic Signaling Pathway, Promotes Prostate Xenograft Tumor Growth. The details of those findings and the appropriate data and graphic representations are all included in that appended text. I anticipate no changes to the original statement of work.

**Key Research Accomplishments:**

- We have shown in a survey of adult human prostate tissues that substantial levels of hedgehog signaling exist in normal hyperplastic and malignant tissue.

- In cancer specimens Shh expression is localized to the tumor epithelium while Gli1 expression is localized to the tumor stroma. This tight correlation between the levels of Shh and Gli1 expression would suggest active signaling between the tissue layers.

- We have shown that Shh expressed by LNCaP cells in the xenograft tumor model activates Gli1 expression in the tumor stroma.

- Shh over expression in LNCaP cells accelerates tumor growth. This is associated with a dramatic up-regulation of stromal Gli1 expression. Together these implicate Shh as an important paracrine activator in prostate cancer.

**Reportable Outcomes:**

1) A manuscript describing these results has been submitted for publication (appended).

2) Based on this work a post-doctoral fellow, Mark Koeppel has applied for and received funding from the Department of Defense.

**Conclusions:**

This work has identified, for the first time, Shh signaling as an important paracrine activator in prostate cancer growth. Our studies have shown that this signaling pathway is active in human prostate cancer and that it dramatically accelerates tumor growth in a xenograft model. As Shh signaling is a demonstrated target for chemical inhibition and has significant chemotherapeutic applications in cancer, these finding have great importance for human health. They identify Shh signaling as a potential target for therapeutic intervention to slow or arrest prostate tumor growth – and provide patients with prostate tumor growth extended life expectancy and increased quality of life. Toward validating this goal, we are pursuing the remaining goals of the work as previously outlined. Namely, we intend to test whether Shh loss of function in LNCaP stromal cells inhibits tumor formation and growth.

# Hedgehog Signaling, an Embryonic Signaling Pathway, Promotes Prostate Xenograft Tumor Growth

Lian Fan[1,2], Carmen V. Pepicelli[1,3], Christian C. Dibble[3], Winnie Catbagan[4], Jodi L. Zarycki[3], Robert Laciak[5], Marilyn L.G. Lamm[4], Alejandro Munoz[6], J. Brantley Thrasher[7] and Wade Bushman[6,8]

[1]Both authors contributed equally to this work
[2]Current address: Global Toxicology, Pharmacia Corporation, 4901 Searle Parkway, Q2628, Skokie, IL
[3]Curis, Inc., Oncology Group, 45 Moulton Street, Cambridge, MA
[4]Current address: Children's Memorial Institute for Education and Research, Northwestern University Feinberg School of Medicine, Chicago, IL
[5]Current address: University of Illinois College of Medicine, College of Medicine West,1853 West Polk Street, Chicago, IL
[6]Division of Urology/Department of Surgery, University of Wisconsin, G5/350 Clinical Sciences Center, 600 Highland Avenue, Madison, WI
[7]Division of Urology, University of Kansas Medical Center, 3901 Rainbow Blvd, Kansas City, KS
[8]Correspondence should be addressed to bushman@surgery.wisc.edu

Category: Carcinogenesis or Tumor Biology

Running title: Hedgehog signaling in prostate tumors

Keywords: prostate cancer, sonic hedgehog, Patched, Gli, epithelial-stromal interactions

**ABSTRACT**

During fetal prostate development, Sonic hedgehog (*Shh*) expression by the urogenital sinus epithelium activates *Gli-1* expression in the adjacent mesenchyme and induces ductal budding and growth. *Shh* signaling is down regulated at the conclusion of prostate ductal development. However, a survey of adult human prostate tissues reveals substantial levels of Shh signaling in normal, hyperplasic and malignant prostate tissue. In cancer specimens, the *Shh* expression is localized to the tumor epithelium, while *Gli-1* expression is localized to the tumor stroma. Tight correlation between the levels of *Shh* and *Gli-1* expression suggests active signaling between the tissue layers. To determine whether *Shh-Gli-1* signaling could be functionally important for tumor growth and progression, we performed experiments with the LNCaP xenograft tumor model and demonstrated that: (1) *Shh* expressed by LNCaP tumor cells activates *Gli-1* expression in the tumor stroma, (2) genetically engineered *Shh* overexpression in LNCaP cells leads to increased tumor stromal *Gli-1* expression and (3) *Shh* overexpression dramatically accelerates tumor growth. These data suggest that hedgehog signaling between the epithelial-derived prostate cancer cells and stroma may be a critically important factor in growth of some human prostate cancers.

## INTRODUCTION

### Stromal-epithelial interactions in prostate cancer

The prostate is a glandular tissue composed of secretory epithelial parenchyma and stroma that consists primarily of smooth muscle cells and fibroblasts (1,2). These stromal cells elaborate the components of the extra cellular matrix, including collagen, elastic fibers and matrix associated growth factors, as well as other signaling molecules that regulate cell proliferation and differentiation (3). Tissue recombination studies demonstrated the role of mesenchyme in directing growth and morphogenesis during embryonic prostate development (4), and a growing body of evidence indicates that stromal cells play an equally intimate role in the process of cancer development and progression (5,6).

The cell components of the stroma in prostate cancer are similar to those in the normal prostate. However, a variety of experimental observations indicate that the stroma may undergo phenotypic and/or genotypic changes that can enhance prostate tumor progression. Co-injection of prostate cancer derived prostate fibroblasts with tumorogenic epithelial cells enhances tumor take and growth in nude mice (7-11). Similarly, human fibroblasts obtained from prostate tumors promote tremendous growth when mixed with SV40-T immortalized human prostatic epithelial cells and grafted under the kidney capsule of athymic mice (12). It has been suggested that the stromal reaction in cancer is a permutation of the generalized role of stromal cells in wound healing and that this response, elicited in response to tumor cells, may inadvertently create conditions which favor tumor progression (3). Likewise, tumors may recruit

normal stromal fibroblasts to contribute to tumor growth by inducing a variety of angiogenic and growth factors in a paracrine fashion (reviewed in 13).

**Hedgehog proteins in the prostate**

Sonic hedgehog (Shh), a secreted signaling protein, is one of three mammalian homologs of the Drosophila gene hedgehog expressed during prostate development (14-17). It acts as a potent inducer of morphogenesis and growth in diverse structures of the developing embryo (18,19). All known biologic activity is associated with the N-terminal fragment of the protein (20,21), which undergoes lipid modification in the form of covalent coupling with cholesterol (22) after cleaveage from the C-terminus and secretion. This process is believed to restrict its diffusion and range of action.

Shh exerts its effects by activating gene transcription in target cells expressing the hedgehog receptor Patched (Ptc-1; 23) which is often expressed adjacent to the cells producing Shh (24,25). This interaction initiates a complex intracellular signal transduction cascade that activates the transcription factor *Gli-1* (26), one of three mammalian *Gli* genes related to the Drosophila segment polarity gene Cubitus interruptus (27). *Gli-1* activation results in increased expression of *Gli-1* itself, the *Shh* receptor *Ptc-1*, and target genes, which regulate proliferation, differentiation, and extra cellular matrix interactions (28). *Gli-2* encodes a transcriptional regulator that shares extensive homology with *Gli-1* and may provide functional redundancy in the transcriptional response to Shh signaling. *Gli-3* is believed to provide both positive and negative regulatory control over the expression of *Shh* target genes (reviewed in 29).

Our studies of prostate development identified Shh as a critically important signal linking epithelium and mesenchyme in the induction of ductal morphogenesis (15). *Shh* expression in the epithelium of the developing prostate concentrates at sites of ductal bud formation and the tips of the growing ducts. *Shh* activates *Gli-1* expression in the adjacent mesenchyme. Shh similarly up regulates mesenchymal expression of *Gli-2*. Antibody blockade or chemical inhibition of *Shh* signaling impairs the activation of *Gli-1* expression and inhibits ductal budding and growth (14-15). Since this effect entails primarily an inhibition of epithelial cell proliferation, it suggested that epithelial *Shh* expression activates stromal mediated paracrine signals that feed back and stimulate epithelial cell proliferation. *Shh* and *Gli-1* expression parallel the process of ductal morphogenesis and are down regulated after prostate development is completed. An initial survey of adult human prostate specimens revealed abundant *Shh* and *Gli-1* expression in the majority of human prostate cancers. This observation prompted us to examine the effect of *Shh* overexpression on growth of the LNCaP xenograft tumor.

LNCaP cells are human prostatic epithelial cells derived from a metastatic supraclavicular lymph node (30). The LNCaP cell line forms xenograft tumors at high efficiency when co-injected with Matrigel into nude mice (31). The xenograft tumors are composed of (human) LNCaP prostate cancer cells and host (mouse) derived stromal cells. We have taken advantage of this model to examine the influence of *Shh* signaling on prostate tumor growth. Our studies show that *Shh* expressed by LNCaP cells activates *Gli-1* gene expression in host derived stromal cells and that overexpression of *Shh* in the

prostate cancer cells up regulates *Gli-1* gene expression *in vivo* and accelerates xenograft prostate tumor growth. All of the evidence suggests that *Shh* acts through the stroma to stimulate tumor cell proliferation, presumably by activating paracrine signaling mechanisms. Taken in conjunction with our companion studies of *Shh* and *Gli* gene expression in human prostate cancer, these observations identify *Shh* signaling as a mechanism by which prostate cancer cells may recruit stromal cells to support prostate tumor growth.

## MATERIALS AND METHODS

### Plasmids and cell lines

The human *Shh* overexpression vector, pIRES2-h*Shh*-EGFP was made by cloning a 1.55Kb human *Shh* cDNA fragment (provided by Dr. Cliff Tabin, Harvard University) into the EcoRI site of pIRES2-EGFP mammalian cell expression vector (Clontech) and confirming orientation by restriction endonuclease digestion. LNCaP cells (ATCC, Rockville, MD) were transfected with pIRES2-h*Shh*-EGFP or with pIRES2-EGFP vector alone using Lipofectin (Gibco BRL) and selected with 0.4 μg/ml G418 (Gibco BRL) in culture medium consisting of RPMI-1640 (Gibco BRL) supplemented with 10% fetal bovine serum (FBS), penicillin (100 U/ml) and streptomycin (100 μg/ml. Cells were subcloned by limiting dilution and clones were identified by flow cytometry using the GFP tag. One high *Shh* expressor clone (designated LNCaP$^{Shh(H)}$) and one medium *Shh* expressor clone (designated LNCaP$^{Shh(M)}$) were identified by different levels of GFP expression with flow cytometry and their *Shh* expression levels were confirmed by real time RT-PCR and Western blot analysis. Cell proliferation *in vitro* was quantitated by comparing cell counts using a coulter counter on replicate platings at different time points.

### Xenograft model

All animal experiments were conducted in accord with institutional policies and IAUCC guidelines. LNCaP xenograft tumors were created by subcutaneous co-injection of LNCaP cells ($1x10^6$ in 250 μl PBS) with 250μl Matrigel into both flanks of adult male nude CD-1 mice (Charles River Laboratories). Ten mice each were injected with each of the four cell lines. Tumors were measured weekly with a caliper and tumor volumes were

calculated according to the formula (Length x Width x Depth x 0.5236; 32 ; Note: Volume= $\pi \times W \times D \times L/6$ is the volume of an ellipsoid.). The mice were followed for eleven weeks, although some cell lines experienced high mortality beginning at week nine. All procedures were approved by the Animal Care and Use Committee of Northwestern University.

**RT-PCR**

Expression levels of *Shh* and *Gli* in the initial study were determined by semi-quantitative RT-PCR performed as previously described (16), using message for the ribosomal subunit protein, *RPL-19*, as an internal standard. RNA samples were amplified for 35 cycles. The annealing temperature for all PCRs was 60°C, except for mouse *Ptc-1*, which was 64°C. Sequences for primers and length of the products are as follows:

human *Shh* forward 5' AGA GTA GCC CTA ACC GCT CC 3' and reverse 5' GGC TTC AGC TGG ACT TGA CC 3' 160bp

mouse *Shh* forward 5' GGC AGA TAT GAA GGG AAG AT 3'and reverse 5' ACT GCT CGA CCC TCA TAG TG 3' 260bp

mouse *Patched-1*forward 5' GCA TTC TGG CCC TAG CAA TA 3'and reverse 5' GTC TCA GGG TAG CTC TCA TA 3' 228bp

human *Gli-1*forward 5' GCT AGA GTC CAG AGG TTC AA 3' and reverse 5' CAG TAG GTG GGA AGT CCA TA 3' 229bp

mouse *Gli-1* forward 5' CCT GCT CAG CAC TAC ATG CT 3'and reverse 5' TGT GGC GAA TAG ACA GAG GT 3' 314bp

mouse *Gli-2* forward 5' TTC ATG GAG TCC CAG CAG AA 3'and reverse 5' CTG GCC ATA GTA GTA TAG CG 3' 273bp

mouse *Gli-3*forward 5' AGG TGA CCT GTC AGG TGT AG 3'and reverse 5' TGA AGC ATC TGT GGA GAT GG 3' 220bp

human *RPL-19* forward 5' GTG GCA AGA AGA AGG TCT GG 3' and reverse 5' ATG ATC TCC TCC TTC TTG GC 3' 505bp

mouse *RPL-19* forward 5' TCA GGC TAC AGA AGA GGC TT 3'and reverse 5' GAC AGA GTC TTG ATG ATC TC 3' 556bp

Expression levels of *Shh* and *Gli-1* in further human expression studies and xenograft tumors were determined by quantitative RT-PCR using TaqMan instrumentation (Applied Biosystems). Total RNA was isolated from cryo-pulverized tissue with Trizol (GIBCO-BRL) according to the manufacturer's instructions. RNA was then subjected to reverse transcription using standard protocols. Species-specific primers for human *Shh* and mouse *Gli* genes and *Ptc-1* were used to localize expression to the epithelial and mesenchymal components of the xenograft tumor. Real-time RT-PCR analysis used gene-specific primers and fluorescent probes for Hedgehog pathway genes and glyceraldehydes-3-phosphate dehydrogenase (GAPDH) as an internal standard. Each PCR reaction was run in duplicate and according to the manufacturers recommendations and default settings.

human *GAPDH* forward 5' CCA CAT CGC TCA GAC ACC AT 3'; reverse 5' GCA ACA ATA TCC ACT TTA CCA GAG TTA A 3'; probe FAM-CGC CCA ATA CGA CCA AAT CCG-TAMRA

human *Shh* forward 5' AAG GAC AAG TTG AAC GCT TTG G 3'; reverse 5' TCG GTC ACC CGC AGT TTC 3'; probe VIC-CTC CTG GCC ACT GGT TCA TCA CCG-TAMRA

human *Ptc-1* forward 5' CGC TGG GAC TGC TCC AAG T 3'; reverse 5' GAG TTG TTG CAG CGT TAA AGG AA 3'; probe VIC-CCG ATC AAT GAG CAC AGG CCC A-TAMRA

human *Gli-1* forward 5' AAT GCT GCC ATG GAT GCT AGA 3'; reverse 5' GAG TAT CAG TAG GTG GGA AGT CCA TAT 3'; probe VIC-CCC ACC ATG GAG GTC CCA ACT TCT G-TAMRA

human *Gli-2* forward 5' AAG AAA GTG ATG ATG CGA TGT CTA A 3'; reverse 5' TGT CGG TAA AGC AGC ACA TGT AT 3'; probe: VIC-ACG TTC AAG GCA CCG CAT CTG TGA TC-TAMRA

human *Gli-3* forward 5' ATC ATT CAG AAC CTT TCC CAT AGC 3'; reverse 5' TAG GGA GGT CAG CAA AGA ACT CAT 3'; probe: VIC-CCT CCC GCC TCA CCA CGC CT-TAMRA

mouse *GAPDH* forward 5' AGC CTC GTC CCG TAG ACA AAA T 3'; reverse 5' CCG TGA GTG GAG TCA TAC TGG A 3'; probe FAM-CGG ATT TGG CCG TAT TGG GCG-TAMRA

mouse *Shh* forward 5' AAT GCC TTG GCC ATC TCT GT 3'; reverse 5' GCT CGA CCC TCA TAG TGT AGA GAC T 3'; probe VIC-CGC AGC TTC ACT CCA GGC CAC TG-TAMRA

mouse *Ptc-1* forward 5' CTC TGG AGC AGA TTT CCA AGG 3'; reverse 5' TGC CGC AGT TCT TTT GAA TG 3'; probe VIC-AAG GCT ACT GGC CGG AAA GCG C-TAMRA

mouse *Gli-1* forward 5' GGA AGT CCT ATT CAC GCC TTG A 3'; reverse 5' CAA CCT TCT TGC TCA CAC ATG TAA G 3'; probe VIC-CTC AAG ACG CAC CTT CGG TCG CAC-TAMRA

mouse *Gli-2* forward 5' TCC ATG AAG CTC GTC AAG GTT 3'; reverse 5' GCA AGT AAC TGA GGA GAC TAC AAT ATC C 3'; VIC-TGC GCC TTT CTC CTC CGT GGT G-TAMRA

**Western blots**

For Western blot analysis of *Shh* protein, cells growing in flasks were washed with phosphate buffered saline (PBS) and scraped into 1 ml of lysis buffer (50 mM Tris-HCl, pH 7.5, 150 mM NaCl, 10 mM EDTA, 0.5% deoxycholate, 0.1% SDS, 1% Igepal CA 630, 1 mM sodium vanadate, 10 μg/ml each of aprotinin, leupeptin, and pepstatin), incubated at 4°C for 60 min with gentle shaking and spun for 20 min at 20,000g to obtain clear lysates (33). Tumor tissues were minced into small pieces and homogenized with a glass homogenizer in lysis buffer. Total protein in lysates was quantitated using Biorad protein assay reagent and 10-20 μg protein was run on 14% SDS-PAGE gel, transferred to nitrocellulose membrane (Amersham Corp.), incubated with 1:200 goat anti-human Shh N-terminal antibody (Santa Cruz Cat# SC-1194) followed by 1:5000 horseradish peroxidase-conjugated donkey anti-goat IgG (Santa Cruz Cat# SC-2056) and developed by enhanced chemiluminescence using the ECL reagent according to manufacturer's directions (Amersham Corp.).

**Histology**

Tumor tissues were fixed in 4% paraformaldehyde overnight at 4°C, embedded in paraffin, sectioned at 5μm and stained with hematoxylin and eosin.

**Radioactive *in situ* hybridization**

In situ hybridizations were performed on paraformaldehyde-fixed, paraffin-embedded histological sections, essentially as described in Wilkinson et al. (34). Briefly, 7μm sections were cleared, re-hydrated, digested with proteinase K, acetylated and hybridized with [$^{33}$P]- labeled RNA probes over night. After high stringency post-hybridization washes, slides were dipped in photo emulsion and incubated in the dark for 14-21 days at 4°C. After developing, slides were counter-stained lightly with hematoxylin and imaged under dark-field illumination. Using Photoshop software, dark-field images were artificially colored in red and superimposed onto the corresponding bright-field images. Sense and antisense probes, probe vector used were as follows: human *Shh* (35), human *Ptc-1* (36) mouse *Ptc-1* (25), mouse *Gli-1* and *Gli*-2 (27).

***Gli*-luc assay**

C3H10T1/2 cells (ATCC, Rockville, MD) carrying a hedgehog-responsive reporter gene construct (37) were grown in DMEM with 10% FBS, penicillin/streptomycin, and added glutamine. To assess hedgehog induction by the LNCaP cell lines, these reporter cells were co-cultured with either LNCaP or LNCaP$^{Shh(H)}$ cells, respectively (10,000 each per well) over night in medium containing 10% FBS. The next day, the plates were changed to medium with 0.5% FBS. After 48 hrs, plates were assayed for luciferase activity with the LucLiteTM kit (Packard).

**Human tissues**

Pooled fetal prostate RNA is from 20-22 week old samples and was obtained from ResGen. Adult human prostate tissues were obtained at Northwestern University from the following sources: (1) Normal prostate tissues were obtained from organ donors at the time of organ harvest. (2) Prostate cancer tissues were obtained either by transurethral surgery (channel TURP) in men with clinically advanced prostate cancer or at the time of radical prostatectomy by focal excision of the tumor tissue from prostate specimen. (3) BPH tissues were obtained from specimens at the time of transurethral or open surgery. In each case, the diagnostic designation was histologically confirmed. Paired prostate cancer/ benign prostate tissue specimens were provided by the Tissue and Serum Repository, Kansas Cancer Institute, University of Kansas Medical Center. These specimens were obtained from men undergoing radical prostatectomy for clinically localized prostate cancer. After removal of the specimen, core biopsies were performed of the apparent site of the tumor and the equivalent site on the contralateral side of the specimen. Of the twenty specimens processed in this way, eleven pairs of tumor and benign tissue from the same patient were confirmed by histologic examination. Only these 11 sets were included in the final analysis. All procedures for tissue acquisition and analysis were approved by the IRBs of Northwestern University and Kansas University Medical Center.

**Statistical Analysis:**

*Cell Line Growth Culture:* To assess whether there were any differences in the growth of the four cell lines (LNCaP, LNCaP-GFP, LNCaP$^{Shh(M)}$) LNCaP$^{Shh(H)}$), a Gompertz growth model was fitted to each line. Day 0 cell counts were used as a baseline, so counts for each line in subsequent days were expressed as percentages with respect to the day 0

average count. Natural (base e) logarithms of the percentages were obtained in order to make the variability across time and cell lines more homogeneous.

The Gompertz model is given by: $\ln(\%\ growth) = a \exp(b\ c^t)$, where "ln" denotes the natural logarithm, $t$ is the time (in days), $a$ is the growth limit as $t$ assumes arbitrarily large values, $b$ is related to growth at time 0, and $c$ is the growth rate. The model can accommodate line-specific asymptotes by including dummy variables for each cell line:

$$\ln(\%\ growth)=[a+ag\ \mathrm{GFP}+am\ \mathrm{Med}+ah\ \mathrm{High}]\ \exp(-b\ c^t),$$

where GFP equals one if a given observation is from cell line $\mathrm{LNCaP}^{GFP}$, and 0 otherwise, and Med and High areas are defined similarly. The excluded level (LNCaP) is the reference value. Any significance in the parameters associated with the dummy variables (*ag, am, ah*) captures deviations of those levels with respect to LNCaP. Similarly, the Gompertz model can accommodate line-specific growth rates by expanding $b$ in the original model to a sum of dummy variables with their accompanying coefficients. Since growth is expressed as a percentage relative to day 0 data, it is not meaningful to allow $b$ to vary by cell line.

A Gompertz model with line-specific asymptote and growth rate was estimated via Gauss-Newton optimization, as implemented in R v1.6.2 (38). Model assumptions were assessed via residual plots, and, if warranted, parameter significance was tested via the approximate $t$ test. Non-significant parameters were excluded and the model was re-fit.

*Mice Tumor Growth:* Tumor size ($mm^3$) was plotted against the number of weeks for each mouse, with both sides combined. Mice that failed to reliably establish a tumor were not included in the analysis. Since straight lines provided a reasonably accurate summary representation of the growth patterns, least squares fits were obtained for each mouse by regressing tumor size at each time point and combining both sides. To assess differences between cell line growth, the slopes of the regression lines were analyzed via a one-way nonparametric ANOVA (Kruskal Wallis) by ranking the slopes and performing an ANOVA on the ranks. All six pair wise comparisons between the cell least-squares mean rank were performed.

*Human Tissues:* The expression of Sonic hedgehog (*Shh*) and three related genes (*Gli-1, Gli-2, Gli-3*) were measured by real time RT-PCR analysis in two sets of tissues from adult males. Data set 1 (DS1) consisted of nineteen adult male prostate specimens obtained at Northwestern University that were classified into three groups by clinical diagnosis, histologically confirmed normal (N; n=7), prostate cancer (PC; n=6) and benign prostatic hyperplasia (BPH; n=6). Data set 2 (DS2) consisted of tissues obtained at the University of Kansas Medical Center. Although data from DS1 and DS2 were obtained from different sources and analyzed in different RT-PCR reactions, they were combined for the statistical analysis. Differences in the mean gene expression between groups were tested with a one-way analysis of variance (ANOVA; completely randomized design). The residuals were examined for evidence of violations in the assumptions. If needed, variance-stabilizing transformations were used. If the overall P-value for the ANOVA was significant, pair-wise contrasts were obtained for all possible

group pairs. No adjustment was made for testing all contrasts. DS1 and DS2 were combined to yield a set containing the following samples: normal prostate (N, n=7), benign prostatic hyperplasia (BPH, n=6), prostate cancer (PC, n=6), tumor (T, n=11), and benign (B, n=11). Notice that each individual in DS1 contributes one observation to the combined data set. In contrast, each individual in DS2 contributes two observations to the joint data set. No adjustment was made for this asymmetry.

To assess whether *Shh* should be incorporated as a covariate, analysis of covariance (ANCOVA) was used for each of the three *Gli* genes. The model allowed for the possibility of differences in the intercept and the slope across groups. Model fit diagnostics were obtained via graphical assessment of the residuals. If warranted, transformations were used to ensure the model assumptions were not violated.

The plots and Gompertz fits were generated in R version 1.6.25.1 (38). The ANOVA, and ANCOVA and Kruskal-Wallis analyses models were fit in SAS, release 6.12 (39).

## RESULTS

**Expression of *Shh* and *Gli* in the human prostate: normal, BPH and cancer.**

*Shh* is expressed in the human fetal prostate. Expression is most abundant between 11 and 16 weeks of gestation, a period of ductal budding and intense ductal morphogenesis, and is markedly diminished by 34 weeks of gestation (16). An initial semi-quantitative RT-PCR survey of *Shh* expression in 3 normal adult prostate specimens (18, 30 and 45 years), and 8 specimens of high grade (Gleason 8-10) prostate carcinoma, including 2 hormone refractory tumors, revealed low expression in normal prostate specimens and apparently increased *Shh* expression in the majority of the cancer tissues. A representative gel is shown **(FIGURE 1)**. A companion survey of *Gli-1* expression showed increased *Gli-1* expression in all 8 cancer specimens examined and an apparent correlation between the intensity of *Shh* and *Gli-1* expression in the individual specimens. The levels of *Shh* and *Gli-1* expression in these tumor specimens are comparable to the level of expression observed in the 15.5 week fetal prostate (data not shown). These data suggest that *Shh* and *Gli-1* are frequently and coordinately up-regulated in prostate cancer.

To more comprehensively characterize *Shh* and *Gli* gene expression in the human prostate, two subsequent surveys were performed. The first compared *Shh* and *Gli* gene expression in 7 normal prostate (N) specimens from organ donors 15-28 years old, 6 benign prostatic hyperplasia (BPH) specimens obtained by TURP (n=4) or open prostatectomy (n=2), and 6 prostate cancer (PC) specimens obtained from glands removed by radical prostatectomy. The purpose of this survey design was to compare

gene expression in normal prostate tissue from young adult men (N), in hyperplastic (benign) tissue from men without prostate cancer (BPH) and in specimens of human prostate cancer (PC). Expression of *Shh*, *Gli-1*, *Gli-2*, and *Gli-3* was assayed by quantitative real time RT-PCR. Since the hedgehog pathway is typically down-regulated to maintenance or undetectable levels in most adult organs, expression was normalized to an internal expression standard of robust developmental *Shh* signaling activity, fetal brain RNA. This survey revealed that *Shh* expression is generally abundant in both benign (N and BPH) and cancer (PC) specimens (**FIGURE 2**). For statistical analysis of expression in the different groups, logarithmic and rank transformations were used in order to satisfy the assumptions of normality and homogeneous variance across groups. There was little difference between the two, so only the results for the logarithmically-transformed (base *e*) expressions are shown (**FIGURE 2A, B**). Analysis of variance (ANOVA) revealed no significant differences in levels of *Shh* expression (P=0.991)or *Gli-1* expression (P=0.802) in the normal (N) and BPH specimens (Fig. 2A), although expression of *Gli-2* and *Gli-3* between these two groups differs significantly (Fig.2A; P=0.007 and P=0.018, respectively). There seemed to be increased *Shh* and *Gli-1* expression in the cancer specimens (PC) as compared to normal (N) and BPH, but the differences were not statistically significant (P=0.263 and P=0.251 for *Shh* and P=0.161 and P=0.226 for *Gli-1*, respectively). Recognizing that the best control for any individual prostate cancer specimen may be benign tissue from the same gland, a second survey was performed to compare expression in prostate cancer and in zone-homologous non-malignant prostate tissue from the same gland. Paired specimens of tumor (T) and benign (B) tissue from 11 men undergoing radical prostatectomy were obtained by matching histologically

confirmed tumor with histologically confirmed benign tissue obtained from the contralteral lobe. Statistical analysis revealed no significant differences in *Shh* or *Gli* gene expression between the cancer specimens and zone homologous tissues from the same group of patients (Fig. 2A, T vs B; P=0.4645). While these studies do not demonstrate a consistent, statistically significant increase in Shh or Gli-1 gene expression specifically in prostate cancer, they do show that a subset of cancer and benign tissues in both series display extremely high levels of Shh and Gli-1 expression (i.e. one to two orders of magnitude higher than average).

**Active Shh signaling between epithelium and stroma**

The conserved role of *Shh* in activating *Gli-1* expression prompted us to examine whether the level of *Shh* expression predicted the level of *Gli-1* expression in individual specimens. Analysis of co-variance (ANCOVA; **FIGURE 2B**) revealed a highly significant association between *Shh* and *Gli-1* expression (P=0.0001). This association is equivalent in all subgroups and suggests that *Shh* activity determines the expression of *Gli-1*, even in the absence of normalizing for the proportion of epithelium to mesenchyme in the tissues. *In situ* hybridization demonstrated that *Shh* expression localizes to the epithelium, whereas *Gli-1* is expressed by the stroma **(FIGURE 3)**. This finding suggests that stromal *Gli-1* expression is driven by *Shh* signaling from the epithelium. Analysis of covariance also revealed a similarly linear relationship between *Shh* expression and that of *Gli-2* and *Gli-3* **(FIGURE 2B).**

To determine whether the level of *Shh* and *Gli-1* identified in the human prostate tumor specimens is physiologically significant, we compared their expression to that seen in

fetal brain where *Shh* signaling is known to play a critically important role in stimulating growth. Expression of *Shh* and *Gli-1* in matched specimens from patients with prostate cancer (T and B) was typically the same order of magnitude as the fetal brain , but was markedly increased in some cases (**FIGURE 4**). The high level of *Shh* signaling activity in these tissues, in many cases higher even than that of developing embryonic prostate, is consistent with a possible role in tumor growth. The correlation between relative levels of *Shh* and *Gli-1* expression in individual specimens suggested by the statistical analysis is clearly evident in this graphic display [Compare relative levels of *Shh* expression in **FIGURE 4A** and to *Gli-1* expression in **FIGURE 4B** in corresponding specimens].

**LNCaP *Shh* expression is associated with mouse *Gli-1* expression in xenograft tumors**

LNCaP is an androgen responsive human prostate cancer cell line which forms xenograft tumors in nude mice when co-injected with Matrigel, a solubilized membrane preparation rich in extra cellular matrix proteins (30,31). To examine the role of *Shh* in LNCaP xenograft tumor formation and growth, we engineered LNCaP cells to over express human *Shh*. LNCaP cells were stably transfected with a GFP expression vector containing the human *Shh* cDNA under the control of a CMV promoter. Two clones exhibiting different degrees of *Shh* over expression ($LNCaP^{Shh(M)}$ and $LNCaP^{Shh(H)}$) by RT-PCR and Western blot analysis, as compared to a clone transfected with vector only ($LNCaP^{GFP}$) and the parent cell line, were selected for further study. The overexpresser and control cells exhibited identical morphology (not shown), and no significant differences in growth rate ($P>0.112$) or maximal growth ($P>0.739$) in culture **(FIGURE 5).** This argues against any autocrine effect of *Shh* overexpression on growth of the

LNCaP cells. Furthermore, *Shh* over expression is not associated with activation of human *Ptc-1*, *Gli-1 or Gli-2* in monolayer culture (**FIGURE 6**), again arguing against autocrine signaling activity. In addition, a co-culture assay using a *Gli*-luciferase reporter cell line (37) demonstrated robust three- to fourfold induction of luciferase activity by the LNCaP overexpresser cells as compared to the control cell line **(FIGURE 7).** This assay verified that Hedgehog protein is not only expressed and produced, but also properly processed and secreted in the engineered cell lines.

When co-injected with Matrigel, LNCaP parent and Shh overexpresser cell lines form xenograft tumors consisting of nests of human prostate cancer cells and an intervening, well-vascularized fibroblastic stroma derived from the host mouse (31). Xenograft tumors made with *Shh* overexpressing cells and control LNCaP cells appeared indistinguishable (**FIGURE 8**) and review by a urologic pathologist identified no differences in histologic appearance between the tumors made with the LNCaP parent cell line or cells overexpressing Shh. A specific advantage of the xenograft model for studying the role of *Shh* signaling is that it allows for discrimination of mouse- and human-specific gene expression by use of species specific PCR primers. Human and mouse specific primers were designed and used to assay for *Ptc-1*, *Gli-1* and *Gli-2* expression in order to determine the target of *Shh* signaling. Xenograft tumors made with LNCaP parent and overexpresser cell lines show low and high level human *Shh* expression, respectively. In accordance with our cell culture assays, these expression experiments revealed barely detectable human *Ptc-1* expression and no human *Gli-1* expression (not shown). Mouse *Ptc-1* and *Gli-1* were, however, detected in xenograft

tumors made with the LNCaP parent cell line and demonstrated high levels of expression in xenograft tumors made with cells overexpressing the Hedgehog ligand (**FIGURE 9**). These findings indicate that *Shh* secreted by LNCaP cells is signaling to mouse stromal cells present within the xenograft tumor and activating stromal cell *Ptc-1* and *Gli-1* expression only in a paracrine loop. This was confirmed by radioactive *in situ* hybridization on xenograft tumor tissue, in which the hedgehog ligand is expressed by epithelial cells, while the Hedgehog target genes *Ptc-1* and *Gli-1* are expressed in the adjacent stroma (**FIGURE 10**), as is the case in human prostate tumors.

**Shh overexpression accelerates tumor growth.**

It has been demonstrated previously that in order to obtain tumor formation at high frequency, LNCaP cells must be co-injected with either Matrigel or a suitable stromal cell line such as bone fibroblasts. Control cells and LNCaP cells overexpressing *Shh* formed tumors with equally high take rates (80-100%) in multiple experiments. To test whether *Shh* overexpression would ameliorate the requirement for co-injection with Matrigel, control and overpressor cells were injected without Matrigel and tumor formation scored weekly. Neither the control nor *Shh* overexpresser cells demonstrated significant tumor formation even with prolonged (12 week) follow up (data not shown), indicating that epithelial-stromal interactions facilitated by Matrigel are critically important for establishment of xenograft tumors and cannot be overcome by expression of *Shh* alone.

When comparing the growth rate of tumors generated with *Shh* overexpresser and control cells co-injected with Matrigel, a significantly increased growth rate for the tumors made

with LNCaP cells overexpressing *Shh* was observed **(FIGURE 11).** The comparison demonstrates a significantly increased rate of tumor growth for the medium and high *Shh* overexpressers as compared to both the GFP and parent cell line controls. Histologic examination of the tumors excluded an increase in stromal proliferation as an explanation of the increased tumor growth rate, since both overexpresser and control xenografts are composed of an epithelium-rich tumor with a relatively small component of stromal tissue. Taken together, these findings suggest that *Shh* overexpression results in increased tumor growth by stimulating tumor cell proliferation in a paracrine manner.

## DISCUSSION

### Hedgehog signaling in the developing and normal adult prostate

Shh-Gli signaling plays an essential role in ductal morphogenesis during prostate development. *Shh* is expressed by the epithelium of the male urogenital sinus and activates *Gli-1* gene expression in the adjacent mesenchyme (14,15). This occurs coincident with the formation of the epithelial outgrowths (buds) that form the main prostatic ducts. Blockade of Shh signaling inhibits activation of *Gli-1* gene expression and the process of ductal budding. This loss of ductal budding is associated with diminished epithelial proliferation, implicating Shh-Gli signaling as a mechanism that activates Gli-mediated paracrine signals, which in turn promote epithelial proliferation and outgrowth of the ductal tip during embryonic development. *Shh* expression in the prostate diminishes as ductal morphogenesis is completed.

In the postnatal prostate, this signaling pathway appears to play a role in differentiation, rather than cell division, as it induces differentiation of epithelial cells into postmitotic, terminally differentiated luminal cells (17). The apparent contradictory functions of Shh in growth and differentiation of the developing versus postnatal prostate may be due to differing concentrations of the active Shh-N protein or changing tissue responsiveness due to the presence or absence of negative regulators such as activin A and TGF-beta 1 in the stroma (17). Even so, both sets of publications firmly establish the presence of a paracrine signaling mechanism from the Shh expressing epithelium to the stroma, which activates hedgehog-responsive genes such as Ptc-1 and Gli-1 and, presumably, reciprocal mesenchymal signals that affect epithelial cell proliferation and differentiation.

Epithelial-mesenchymal interactions driven by epithelially expressed Hedgehog ligand are a central theme in the morphogenesis of several other developing organs (40-44). As inappropriate activation of more and more developmentally expressed signaling pathways emerges as a key factor in oncogenesis and hyperproliferative disease, (reviewed in 45-47), we decided to examine the expression levels of Hedgehog pathway genes in human prostate cancer and benign prostatic hyperplasia samples. Our survey reveals 1) significant maintenance levels of *Shh* and *Gli* gene expression in the adult human prostate, 2) very high levels of Hedgehog signaling in some cases of prostate cancer and benign prostatic hyperplasia, and 3) a strong correlation of the amplitude of *Shh* with that of *Gli* gene expression, regardless of the relative proportion of epithelium and mesenchyme.

**Hedgehog signaling in diseased prostate tissue**

Analysis of specimens from young adult men, from men with BPH and from men undergoing radical prostatectomy for prostate cancer revealed relatively abundant *Shh* expression in all three groups. There was a trend toward higher *Shh* and *Gli-1* expression in the cancer specimens as a group, with a subset of the samples producing substantially more *Shh* than the average (FIGURE 2A). This was echoed in a subsequent survey of tumors, in which more than half the tumors exhibited expression levels equal to or higher than those of fetal brain. In more than one third of all cases, the amplitude of *Shh* expression was higher than that in developing 22 week fetal prostate (**FIGURE 4**). These studies show that abundant *Shh* expression is not specific to clinically evident

prostate cancer. However, the robust level of signaling may nonetheless be an important factor that enables prostate cancer progression.

We compared expression in histologically confirmed tumor and benign tissue from the same gland in men with localized prostate cancer to determine whether increased *Shh* and *Gli-1* expression is specific to the area of the tumor. This survey showed a wide variation in the levels of *Shh* and *Gli-1* expression among tumors, but a surprisingly strong correlation between expression in the tumor and benign tissue from the same patient. This suggests that the level of *Shh* signaling is either a characteristic of an individual's prostate in general or that non-malignant tissue in prostates affected by malignant growth expresses levels of Shh similar to those of the cancer. The very tight correlation between *Shh* and *Gli-1* expression and the localization of *Shh* and *Gli-1* expression to the epithelium and stroma, respectively, indicates functional signaling by Shh from the tumor cells to the prostatic stroma. This interpretation is buttressed by a survey of commercially available prostate cancer and benign prostatic hyperplasia cell lines which identified some cell lines in which the Hedgehog ligand is expressed at high level, without concomitant expression of *Gli-1* in the same cells (data not shown). Intriguingly, the strong correlation of the amplitudes of *Shh* and *Gli-1* appears independent of the proportion of mesenchymal cells in the tissue that will likely vary from specimen to specimen. This may indicate that, in addition to paracrine signaling into the adjacent stroma, the expression of mesenchymally expressed target genes is perhaps up-regulated on a per-cell basis by oncogenic mutation, in contrast to the situation described in a recent survey of expression of mesenchymally expressed Hedgehog pathway genes (Gli-

1, Ptc-1, Hip-1) in other, non-prostatic types of cancer, in which no up-regulation of Hedghog signaling was found (48). Although there is no evidence that oncogenic mutation of the Hedgehog pathway genes *Ptc-1* or *Smo* exists in prostate cancer, it is nonetheless possible that in some prostate cancers the pathway is up-regulated by inactivation or deletion of negative pathway elements expressed in the stroma, as may be the case for suppressor of fused [Su(fu)], a negative regulator of Hedgehog signaling (49) whose expression typically tracks that of *Gli-1* and *Ptc-1*. Interestingly, loss of heterozygosity of the fragment of chromosome 10 which harbors the Su(fu) gene has been observed in a high percentage of prostate cancers (50,51), as have structural chromosomal aberrations of prostate cancer cell lines in which the breakpoint for translocation is localized immediately upstream of the Su(fu) locus (52). It follows that Su(fu) deletion or translocation may provide an additional means of inappropriately upregulating Hedgehog signaling in an organ which continues to express a maintenance level of Hedgehog protein.

Prostate cancer is frequently a multifocal process – suggesting the operation of one or more factors that promote malignant transformation and/or tumor progression diffusely in the prostate. These factors might include genetic, hormonal, or environmental influences and may not only affect nascent tumor cells but also the stromal context in which tumor formation occurs. Several studies have shown increased levels of aromatase and aminopeptidase A in stromal cells adjacent to prostate carcinoma and shown altered expression of matrix metalloproteinases (MMPs) and tissue inhibitors of metalloproteinases (TIMPs) (3). More recently, changes in stromal cell phenotype have been shown to occur specifically in areas adjacent to proliferative intraepithelial

neoplasia (PIN) and carcinoma (53). The stromal cells associated with human prostate cancer, called either reactive stromal cells (3) or carcinoma-associated fibroblasts (CAF; 12) possess the ability to promote tumor growth *in vivo* (reviewed in 54 and 55). The mechanisms by which stromal cells influence tumor growth are not well defined but are postulated to include angiogenic factors, growth factors and MMPs. The changes that occur in the stroma associated with tumor cells are also not well defined. They are thought to be induced changes, but the mechanism for stromal "activation" is unknown (55). Our finding of abundant Shh signaling activity in adult prostate tissue and in tumors suggests that Shh signaling may be one mechanism by which tumor cells recruit stromal cells to support tumor growth.

**The effects of Hedgehog signaling on prostatic stroma**

To examine the possibility that *Shh* expression by tumor cells modulates their stromal effect on tumor growth, we engineered *Shh* overexpression in the LNCaP xenograft tumor. Overexpression of *Shh* in this cell line is not associated with any changes in Hedgehog target gene expression or cell growth in monolayer culture that would indicate an autocrine effect. Nonetheless, it significantly accelerates tumor growth, primarily due to an increase in tumor cells. Although we can not rule out an increase in stromal cell proliferation, the apparently unaltered histologic appearance of the tumor as an epithelial-rich xenograft juxtaposed with the dramatic increase in growth rate argues for an effect predominantly on the growth rate of the epithelial compartment of the tumor. Examination of human *Ptc-1*, *Gli-1* and *Gli-2* expression confirmed that there is no autocrine Shh signaling activity in the xenografts tumor cells. In contrast, *Shh* overexpression upregulates host cell *Gli-1* expression. It follows that the effect of *Shh*

overexpression on tumor cell proliferation is mediated by Gli-based activation of stromal genes, and as a corollary, paracrine mechanisms which support and contribute to tumor growth. Our observations of analogous Shh-Gli signaling from the epithelium to the mesenchyme in human prostate cancer strengthens the argument that *Shh* is also a critical link in eliciting support and growth inducing signals from the tumor stroma (**FIGURE 12**).

Gli-1 activation has been identified as a major regulator of cell growth. Activating mutations or overexpression can produce cell transformation (56) and Gli-1 over activity has been firmly implicated in the etiology of human basal cell carcinoma (57). Yoon et al. (28) have identified approximately 30 targets of Gli-1, including Cyclin D2, Osteopontin, IGF binding protein 6, MAP kinase 6c, and plakoglobin. Hepatocyte nuclear factor-3beta (HNF-3beta) is another well established target of Gli1 regulation (58). Several members of this battery of *Gli-1*-responsive genes are expressed in the fetal prostatic mesenchyme (unpublished observations), suggesting that Hedgehog signaling may also be critical for the induction of growth related genes such as HNF-3beta, MAP kinase 6c, Osteopontin, IGFBP6, and Cyclin D2 in adult stromal cells. Interestingly, in co-cultures of LNCaP$^{Shh(H)}$ cells with normal fibroblasts and in normal host fibroblasts in xenograft tumors *Gli-1* transcripts reach a plateau of high-level expression, while the Gli-1 level in diseased human prostate tissue is strictly proportional to the level of Shh, indicating that fundamental changes to the stromal cells' ability to negatively regulate the amplitude of Hedgehog signaling have occurred.

Another mechanism by which Hedgehog may recruit stromal cell types for tumor support is by induction of angiogenesis. Hedgehog signaling has recently been shown to play a critical role in the formation of blood vessels in two ways. First, Shh protein induces stromal upregulation of angiogenic factors such as angiopoietin 1 and 2, VEGF and basic FGF (59), allowing for neovasculatization of ischemic tissue. Second, it was shown to directly induce microvessel formation by endothelial cells (60). Conceivably, Hedgehog is a similarly important contributor to vascularization in the human prostate and as a consequence, may influence not only the growth of primary prostate cancer, but also it's formation of metastases.

Many tumors display characteristic patterns of invasion, spread, and metastasis. This is taken to signify that tumor cells grow best in particular stromal environments that provide a "fertile soil". Prostate cancer, for instance, displays a striking predilection for bony metastasis. As cross-signaling between the stroma and epithelium regulates normal prostate development, it is becoming evident that stromal-epithelial cross-talk plays a similar role in tumor progression. This stromal-epithelial dialogue likely incorporates a number of different activities (e.g. angiogenesis) that utilize normal physiologic signaling mechanisms that can be targeted for pharmacologic modulation. We propose that one such pathway uniquely important in the epithelial-stromal communication of prostate cancer is the Shh signaling pathway. Strategies that target critical elements of the stromal response, such as inhibition of angiogenesis, provide exiting novel therapeutic means of arresting or slowing tumor growth. Similarly, strategies to

interfere with tumor cell recruitment of stromal cell support for tumor growth may provide a complementary pathway of therapeutic intervention.

**Hedgehog signaling in cancer**

Recent molecular and genetic studies have demonstrated that ectopic activation of Sonic Hedgehog signaling is a key event in the generation of sporadic (61,62) and hereditary basal cell carcinoma (63,36) as well as medulloblastoma (64,65). Likewise, mice heterozygous for Ptc-1 develop medulloblastomas (66) and, under some experimental conditions, skin lesions resembling basal cell carcinoma (67). In these cancers, activation of the Hedgehog pathway is believed to induce proliferation in epithelial tumor cells via activation of cyclins and cyclin-dependent kinases (68) in an autocrine loop. Accordingly, Hedgehog antagonists are effective inhibitors of tumor growth in models of medulloblastoma (69) and basal cell carcinoma (37). Recently, ligand-dependent Hedgehog signaling has been described in a subset of small-cell lung carcinomas (SCLC) and SCLC cell lines tested (70). Tumor growth is significantly inhibited by treatment with the natural product Hedgehog antagonist cyclopamine in a xenograft model derived from one of these cell lines which is expressing Shh and Gli-1 concomitantly. In contrast to the above-mentioned scenarios, we postulate, based on the expression patterns of Shh and downstream target genes in human prostate cancer, and on our observations with Shh-overexpressing xenograft models, an additional, paracrine signaling model for Hedgehog contribution to the growth of human tumors. Our observations are in good accord with previously published work establishing that overexpression of Shh protein alone, even in the absence of oncogenic mutation of Ptc or Smo, can induce neoplastic

transformation of epithelial cells and as a consequence, basal cell carcinoma-like lesions in mouse skin (71).

In summary, Hedgehog signaling appears to play a role in tumorogenesis and growth of a number of cancers and by a growing number of mechanisms. It remains to be seen whether small molecule and natural product inhibitors of Hedgehog signaling (37,72) or a Hedgehog blocking antibody can inhibit growth of prostate cancer xenografts, in which case a Hedgehog antagonist may be a valuable therapeutic for the treatment of prostate cancer in humans.

**ACKNOWLEDGEMENTS**

We would like to thank Dr. James Kozlowski for samples of human prostate tissue obtained at Northwestern University, Dr. Amanda Maw for assistance in obtaining additional samples at Northwestern University, and Jodi Ballanger of the KUMC tissue bank for assistance in obtaining matched pairs of benign and malignant prostate tissue. We thank Drs. Lee Rubin, Stephen Gould and Zhou Wang for discussions and comments on the manuscript, and John Lydon for expert help with histology. We also wish to thank Dr. Terrance Oberley for providing pathologic review of the xenograft tumor specimens.

## REFERENCES


1. McNeal, J.E. Normal histology of the prostate. Am J Surg Pathol *12*(8):619-33, 1988.

2. Castellucci, E., Prayer-Galetti, T., Roelofs, M., Pampinella, F., Faggian, L., Gardiman, M., Pagano, F., Sartore, S. Cytoskeletal and cytocontractile protein composition of stromal tissue in normal, hyperplastic, and neoplastic human prostate. An immunocytochemical study with monoclonal antibodies. Ann N Y Acad Sci. *784*:496-508, 1996.

3. Rowley, D. What might a stromal response mean to prostate cancer progression? Cancer Metastasis Rev. *17*(4):411-9, 1998-99. Review

4. Cunha, G.R., Donjacour, A.A., Cooke, P.S., Mee, S., Bigsby, R.M., Higgins, S.J. and Sugimura, Y. The endocrinology and developmental biology of the prostate. Endocrine Rev 8:338-362 ,1987.

5. Tuxhorn, J. A., Ayala, G. E., and Rowley, D. R. Reactive stroma in prostate cancer progression. J Urol *166:* 2472-2483, 2001.

6. Schor, S.L., and Schor, A. M. Phenotypic and genetic alterations in mammary stroma: implications for tumor progression. Breast Cancer Res *3:* 373-379, 2001.

7. Camps, J.L., Chang, S.M., Hsu, T.C., Freeman, M.R., Hong, S.J., Zhau, H.E., von Eschenbach, A.C., Chung, L.W. Fibroblast-mediated acceleration of human epithelial tumor growth in vivo. Proc Natl Acad Sci U S A. *87*(1):75-9, 1990.

8. Chung, L.W. Fibroblasts are critical determinants in prostatic cancer growth and dissemination Cancer Metastasis Rev 10(3):263-74, 1991.

9. Gleave, M., Hsieh, J.T., Gao, C.A., von Eschenbach, A.C., Chung, L.W. Acceleration of human prostate cancer growth in vivo by factors produced by prostate and bone fibroblasts. Cancer Res *51*(14):3753-61, 1991.

10. Olumi, A.F., Dazin, P., Tlsty, T.D. A novel coculture technique demonstrates that normal human prostatic fibroblasts contribute to tumor formation of LNCaP cells by retarding cell death Cancer Res 58: 4525-30, 1998.

11. Condon, M.S., and Bosland, M.C. The role of stromal cells in prostate cancer development and progression. In Vivo. Jan-Feb;*13*(1):61-5. 1999 Review

12. Olumi A.F., Grossfeld G.D., Hayward S.W., Carroll P.R., Tlsty T.D., Cunha G.R. Carcinoma-associated fibroblasts direct tumor progression of initiated human prostatic epithelium Cancer Res 59: 5002-11, 1999.

13. Hanahan, D., Weinberg, R.A. The hallmarks of cancer. Cell *100*, 57-70. 2000.

14. Podlasek, C.A., Barnett, D.H., Clemens, J.Q., Bak, P.M., Bushman, W. Prostate development requires Sonic hedgehog expressed by the urogenital sinus epithelium. Dev Biol. *209:* 28-39, 1999.

15. Lamm, M.L.G., Catbagan, W.S., Laciak, R.J., Barnett, D.H., Hebner, C.M., Gaffield, W., Walterhouse, D., Iannaccone, P., Bushman, W. Sonic Hedgehog Activates Mesenchymal *GLI1* Expression During Prostate Ductal Bud Formation. *Developmental Biology*, Sep 15;*249*(2):349-366, 2002.

16. Barnett, D. H., Huang, H. Y., Wu, X. R., Laciak, R., Shapiro, E., and Bushman, W. The human prostate expresses sonic hedgehog during fetal development. J Urol. *168:* 2206-10, 2002.

17. Wang, B., Shou, J., Ross, S., Koeppen, H., de Sauvage, F.J. and Gao, W.O. Inhibition of Epithelial Ductal Branching in the Prostate by Sonic Hedgehog Is Indirectly Mediated by Stromal Cells. JBC Papers in Press. Published on March 7, 2003 as Manuscript M300968200.

18. Hammerschmidt, M., Brook, A., and McMahon, A. P. The world according to hedgehog. Trends Genet. *13:*14-21, 1997.

19. McMahon, A.P., Ingham, P. W., and Tabin C. J. Developmental roles and clinical significance of hedgehog signaling. Curr Top Dev Biol. *53:* 1-114, 2003.

20. Bumcrot, D.A., Takada, R., McMahon, A.P. Proteolytic processing yields two secreted forms of sonic hedgehog. Mol. Cell Biol. *15:* 2294-303, 1995.

21. Marti, E., Bumcrot, D.A., Takada, R., and McMahon, A.P. Requirement of 19K form of Sonic hedgehog for induction of distinct ventral cell types in CNS explants. Nature *375:* 322-325, 1995.

22. Porter, J.A., Young, K. E. and Beachy, P.A. Cholesterol modification of hedgehog signaling proteins in animal development. Science *274:* 255-259, 1996.

23. Goodrich, L. V., Johnson, R. L., Milenkovic, L., McMahon, J. A. and Scott, M. P. Conservation of the hedgehog/patched signaling pathway from flies to mice: induction of a mouse patched gene by Hedgehog. Genes Dev *10:* 301-312, 1996.

24. Bellusci, S., Furuta, Y., Rush, M. G., Henderson, R., Winnier, G., and Hogan, B. L. Involvement of Sonic hedgehog (Shh) in mouse embryonic lung growth and morphogenesis. Development *124:* 53-63, 1997.

25. Apelqvist, A., Ahlgren, U., and Edlund, H. Sonic hedgehog directs specialized mesoderm differentiation in the intestine and pancreas. Curr Biol. *7*: 801-804, 1997.

26. Kinzler, K.W., Bigner, S.H., Bigner, D.D., Trent, J.M., Law, M.L., O'Brien, S.J., Wong, A.J., Vogelstein, B. Identification of an amplified, highly expressed gene in a human glioma. Science. Apr 3;*236*(4797):70-73, 1987.

27. Hui, C. C., Slusarski, D., Platt, K. A., Holmgren, R. and Joyner, A. L. Expression of three mouse homologs of the Drosophila segment polarity gene cubitus interruptus, Gli1, Gli-2, and Gli-3, in ectoderm- and mesoderm-derived tissues suggests multiple roles of Sonic hedgehog peptides in the developing chick and mouse embryo during post implantation development. Dev Biol *162:* 402-413, 1994.

28. Yoon, J. W., Kita, Y., Frank, D. J., Majewski, R. R., Konicek, B. A., Nobrega, M. A., Jacob, H., Walterhouse, D., and Iannaccone, P. Gene expression profiling leads to identification of GLI1-binding elements in target genes and a role for multiple downstream pathways in GLI1-induced cell transformation. J Biol Chem. *15:* 5548-5555, 2002.

29. Ingham, P.W. and McMahon, A.P. Hedgehog signaling in animal development: paradigms and principles. Genes Development *15*, 3059-3087, 2001.

30. Horoszewicz, J.S., Leong, S.S., Kawinski, E., Karr, J.P., Rosenthal, H., Chu, T.M., Mirand, E.A., Murphy, G.P. LNCaP model of human prostate carcinoma. Cancer Research *43*:1809-1818, 1983.

31. Lim, D.J., Liu, X.L., Sutkowski, D.M., Braun, E.J., Lee, C., Koslowski, M. Growth of an androgen-sensitive human prostate cancer cell line, LNCaP, in nude mice. Prostate *22*:109-118, 1993.

32. Janek, P., Briand, P., Hartman, H.R. The effect of estrone-progesterone treatment on cell proliferation kinetics of hormone-dependent GR mouse mammary tumors. Cancer Research *35*:3698-3704, 1975.

33. Lamm, M.L.G., Long, D., Goodwin, S.M., Lee, C. Transforming growth factor-□1 inhibits membrane-association of protein kinase C□ in a human prostate cancer cell line, PC3. Endocrinology *138*:4657-4664, 1997.

34. Wilkinson, D. G., Bailes, J. A. and McMahon, A. P. Expression of the proto-oncogene int-1 is restricted to specific neural cells in the developing mouse embryo. Cell *50:* 79-88. 1987.

35. Echelard, Y., Epstein, D. J., St-Jacques, B., Shen, L., Mohler, J., McMahon, J. A., and McMahon, A.P. Sonic hedgehog, a member of a family of putative signaling molecules, is implicated in the regulation of CNS polarity. Cell *75:* 1417-1430, 1993.

36. Johnson, R. L., Rothman, A. L., Xie, J., Goodrich, L. V., Bare, J. W., Bonifas, J. M., Quinn, A. G., Myers, R. M., Cox, D. R., Epstein, E. H. Jr., and Scott, M.P. Human homolog of patched, a candidate gene for the basal cell nevus syndrome. Science *272*: 1668-1671, 1996.

37. Williams, J.A., Guicherit, O.M., Zaharian, B.I., Xu, Y., Chai, L., Wichterle, H., Kon, C., Gatchalian, C., Porter, J.A., Rubin, L.L., Wang, F.Y. Inhibiting the Hedgehog Signaling Pathway Induces Regression of Basal Cell Carcinoma-like Lesions. Proc Natl Acad Sci USA, in press

38. Ihaka, R. and Gentleman, R. "R: A language for data analysis and graphics," Journal of Computational and Graphical Statistics *5:* 299-314, 1996. (Software available at: http://www.r-project.org/)

39. SAS Institute SAS Release 6.12. Cary, NC: SAS Institute, 1996.

40. St-Jacques, B., Dassule. H.R., Karavanova, I., Botchkarev, V.A., Li, J., Danielian, P.S., McMahon, J.A., Lewis, P.M., Paus, R., McMahon, A.P. Sonic hedgehog signaling is essential for hair development. Curr Biol *8*:1058-68, 1058-1068.

41. Litingtung, Y., Lei, L., Westphal, H., Chiang, C. Sonic hedgehog is essential to foregut development. Nat Genet *20*:58-61, 1998.

42. Pepicelli, C.V., Lewis, P.M., McMahon, A.P. Sonic hedgehog regulates branching morphogenesis in the mammalian lung. Curr Biol 8:1083-1086, 1998.

43. Ramalho-Santos, M., Melton, D.A., McMahon, A.P. Hedgehog signals regulate multiple aspects of gastrointestinal development. Development. *127*:2763-2772, 2000.

44. Dassule, H.R., Lewis, P., Bei, M., Maas, R., McMahon, A.P. Sonic hedgehog regulates growth and morphogenesis of the tooth. Development *127*:4775-85, 2000.

45. Kim, H., Muller, W.J. The role of the epidermal growth factor receptor family in mammary tumorogenesis and metastasis. Exp Cell Res *253*, 78-87, 1999.

46. Taipale, J., Beachy, P.A. The Hedgehog and Wnt signaling pathways in cancer. Nature *411*,349-354, 2001.

47. Wetmore, C. Sonic hedgehog in normal and neoplastic proliferation: insight gained from human tumors and animal models. Curr Opin Genet Dev *13*, 34-42, 2003.

48. Hu, Z., Bonifas, J.M., Aragon, G., Kopelovich, L., Liang, Y., Ohta, S., Israel, M.A., Bickers, D.R., Aszterbaum, M., Epstein, E.H. Jr. Evidence for lack of enhanced hedgehog target gene expression in common extracutaneous tumors. Cancer Res. *63*:923-928, 2003.

49. Stone, D.M., Murone, M., Luoh, S., Ye, W., Armanini, M.P., Gurney, A., Phillips, H., Brush, J., Goddard, A., de Sauvage, F.J., Rosenthal, A. Characterization of the human suppressor of fused, a negative regulator of the zinc-finger transcription factor Gli. J Cell Sci. *112*:4437-4448, 1999.

50. Carter, B.S., Ewing, C.M., Ward, W.S., Treiger, B.F., Aalders, T.W., Schalken, J.A., Epstein, J.I., Isaacs, W.B. Allelic loss of chromosomes 16q and 10q in human prostate cancer. Proc Natl Acad Sci U S A. *87*:8751-8755, 1999.

51. Bergerheim, U.S., Kunimi, K., Collins, V.P., Ekman, P. Deletion mapping of chromosomes 8, 10, and 16 in human prostatic carcinoma. Genes Chromosomes Cancer *3*:215-220, 1991.

52. Pan, Y., Lui, W.O., Nupponen, N., Larsson, C., Isola, J., Visakorpi, T., Bergerheim, U.S., Kytola, S. 5q11, 8p11, and 10q22 are recurrent chromosomal breakpoints in prostate cancer cell lines. Genes Chromosomes Cancer 30:187-195, 2001.

53. Tuxhorn J.A., Ayala G.E., Smith M.J., Smith V.C., Dang T.D., Rowley D.R. Reactive stroma in human prostate cancer: induction of myofibroblast phenotype and extracellular matrix remodeling. Clin Cancer Res 8: 2912-23, 2002

54. Cunha G.R., Hayward S.W., Wang Y.Z. Role of stroma in carcinogenesis of the prostate. Differentiation 70:473-85, 2002.

55. Sung, S.Y. and Chung, L.W. Prostate tumor-stroma interaction: molecular mechanisms and opportunities for therapeutic targeting. Differentiation 2002 Dec;70(9-10):506-21

56. Nilsson, M., Unden, A.B., Krause, D., Malmqwist, U., Raza, K. Zaphiropoulos, P.G., Toftgard, R. Induction of basal cell carcinomas and trichoepitheliomas in mice overexpressing GLI-1. Proc Natl Acad Sci U S A. *97*:3438-3443, 2000.

57. Dahmane, N., Lee, J., Robins, P., Heller, P., Ruiz, Altaba A. Activation of the transcription factor Gli1 and the Sonic hedgehog signaling pathway in skin tumors. Nature *389*:876-881, 1997.

58. Sasaki, H., Hui, C., Nakafuku, M., and Kondoh, H. A binding site for Gli proteins is essential for HNF-3beta floor plate enhancer activity in transgenics and can respond to Shh in vitro. Development 124:1313-22, 1997

59. Pola, R., Ling, L.E., Silver, M., Corbley, M.J., Kearney, M., Blake, Pepinsky, R., Shapiro R., Taylor, F.R., Baker, D.P., Asahara, T., Isner, J.M. The morphogen Sonic hedgehog is an indirect angiogenic agent upregulating two families of angiogenic growth factors. Nat Med. *7*, 706-711, 2001.

60. Kanda, S., Mochizuki, Y. Suematsu,T. Miyata,Y., Nomata, K., Kanetake, H. Sonic hedgehog induces capillary morphogenesis by endothelial cells through phosphoinositide 3-kinase. J Biol Chem 278, 8244-8249, 2003.

61. Gailani, M.R., Stahle-Backdahl, M., Leffell, D.J., Glynn, M., Zaphiropoulos, P.G., Pressman, C., Unden, A.B., Dean, M., Brash, D.E., Bale, A.E., Toftgard, R. The role of the human homologue of Drosophila patched in sporadic basal cell carcinomas. Nat Genet. *14*:78-81, 1996.

62. Xie, J., Murone, M., Luoh, S.M., Ryan, A., Gu, Q., Zhang, C., Bonifas, J.M., Lam, C.W., Hynes, M., Goddard, A., Rosenthal, A., Epstein, E.H. Jr, de Sauvage, F.J. Activating Smoothened mutations in sporadic basal-cell carcinoma. Nature *391*:90-92, 1998

63. Hahn, H., Wicking, C., Zaphiropoulous, P.G., Gailani, M.R., Shanley, S., Chidambaram, A., Vorechovsky, I., Holmberg, E., Unden, A.B., Gillies, S., Negus, K., Smyth, I., Pressman, C., Leffell, D.J., Gerrard, B., Goldstein, A.M., Dean, M., Toftgard, R., Chenevix-Trench, G., Wainwright, B., Bale, A.E. Mutations of human homologue of Drosophila patched in the Nevoid Basal Cell Carcinoma Syndrome. Cell *85*, 841-851, 1996.

64. Gorlin, R.J. Nevoid basal-cell carcinoma syndrome. Medicine *66*, 98-113, 1987.

65. Raffel, C. Jenkins, R.B., Frederick, L., Hebrink, D., Alderete, B., Fults, D.W., James, C.D. Sporadic medulloblastomas contain PTCH mutations. Cancer Res. *57*:842-845, 1997.

66. Goodrich, L.V., Milenkovic, L., Higgins, K.M., Scott, M.P. Altered neural cell fates and medulloblastoma in mouse patched mutants. Science *277*:1109-1113, 1997b.

67. Aszterbaum, M., Epstein, J., Oro, A., Douglas, V., LeBoit, P.E., Scott, M.P., Epstein, E.H. Jr. Ultraviolet and ionizing radiation enhance the growth of BCCs and trichoblastomas in patched heterozygous knockout mice. Nat Med. *5*:1285-1291, 1999.

68. Duman-Scheel, M., Weng, L., Xin, S., Du, W. Hedgehog regulates cell growth and proliferation by inducing Cyclin D and Cyclin E. Nature *417*:299-304, 2002.

69. Berman, D.M., Karhadkar, S.S., Hallahan, A.R., Pritchard, J.I., Eberhar,t C.G., Watkins, D.N., Chen, J.K., Cooper, M.K., Taipal,e J., Olson, J.M., and Beachy P.A.

Medulloblastoma growth inhibition by hedgehog pathway blockade. Science 297:1559-61, 2002

70. Watkins, D.N., Berman, D.M., Burkholder, S.G., Wang, B., Beachy, P.A., Baylin, S.B. Hedgehog signaling within airway epithelial progenitors and in small-cell lung cancer. Nature *422*:313-317, 2003.

71. Fan, H., Orom, A.E., Scott, M.P., Khavari, P.A. Induction of basal cell carcinoma features in transgenic human skin expressing Sonic Hedgehog. Nat Med. *3*:788-792, 1997.

72. Cooper, M.K., Porter, J.A., Young, K.E., Beachy, P.A. Teratogen-mediated inhibition of target tissue response to Shh signaling. Science *280*:1603-1607, 1998

**FIGURE LEGENDS**

FIGURE 1

RT-PCR assay of *Shh* and *Gli-1* mRNA in prostate tissue from a 30 year old male and transurethral surgical specimens from 8 patients with prostate cancer was performed using the ribosomal subunit *RPL-19* as an internal standard. Specimens Ca5 and Ca6 are from men treated preoperatively with androgen ablation.

FIGURE 2

(A) Natural logarithms of *Shh, Gli-1, Gli-2* and *Gli-3* gene expression data from RT-PCR analysis for each of the five groups (N, normal prostate; BPH, benign prostatic hyperplasia; PC, prostate cancer; T, tumor and B, benign). The mean value of each group is indicated (+). The two groups of specimens (N, BPH, PC) and (T, B) are analyzed separately because they were obtained from different sources and analyzed in different RT-PCR reactions. P-values are reported for analysis of both experiments combined but no comparisons are made across the two groups. *ANOVA:* Pair-wise comparisons revealed no significant differences in gene expression within groups for *Shh* (P=0.222), Gli-1 (P=0.161) or *Gli-3* (P=0.153). For *Gli-2* there were significant differences, with N different from both PC (P=0.0279) and BPH (P=0.0068). (B) *ANCOVA:* Plots of *log(Shh) vs log(Gli-1), log(Gli-2),* and *log(Gli-3)* to examine the relationship of *Shh* expression to the expression of *Gli-1, Gli-2* and *Gli-3* Least-squares regression lines with group-specific slope and intercept are shown. These lines correspond to the analysis of covariance. The three plots suggest a linear relationship between *Shh* and each of the *Gli* genes. For log(*Gli-1*) the overall slope for log(*Shh*) is highly significant (P=0.0001). The

slopes do not differ across groups (P=0.3015), but the group-specific intercepts do differ (P=0.0357). Therefore, log(*Gli-1*) may be described by log(*Shh*) via a set of parallel straight-lines with different intercepts for each group. Similarly, the slopes for the different groups are not significantly different for *Gli-2* and *Gli-3* (P=0.0853 and P=0.1260, respectively) but both log(*Gli-2*) and log(*Gli-3*) may be described by (*Shh*) as straight line predictor (P<0.0002) with varying intercepts (P<0.001).

FIGURE 3

Radioactive *in situ* hybridization analysis for *Shh* (A) and *Gli-1* (B) in tissue sections from human prostate cancer specimen. *Shh* and *Gli-1* expression (red and pink labeling) localized to the tumor epithelium and periductal stroma, respectively. Expression of the indicated genes was investigated in paraffin sections of primary tumors. Bright-field and corresponding dark-field images were superimposed and radioactive signals highlighted with artificial color.

FIGURE 4

Quantitative RT-PCR comparison of *Shh* expression (A) and Gli-1 expression (B) in matched tumor (hatched) and benign (grey) specimens from patients with prostate cancer. Note the generally abundant level of *Shh* and *Gli-1* expression in the prostate specimens as compared to the human fetal brain control, the very high levels of Hedgehog signaling in matched sets 465 through 490, and the tight correlation between relative levels of *Shh* and *Gli-1* expression in individual specimens.

FIGURE 5

Log-relative growth in culture for four LNCaP cell lines, with Gompertz fit (dotted line). Shh overexpression is not associated with any change in growth rate in culture.

FIGURE 6

*Shh* overexpression is not associated with autocrine stimulation of *Ptc-1*, *Gli-1* or *Gli-2* expression in the LNCaP cells. (A) Shh expression in the LNCaP parent cell line by quantitative RT-PCR is low relative to the embryonic brain control (which equals 1 and is too low to be visible in this graph). Shh expression in LNCaP$^{Shh(M)}$ and LNCaP$^{Shh(H)}$ cell lines is approximately three orders of magnitude greater than embryonic brain. *Gli-1* expression is undetectable both in the parent and overexpresser cell lines (data not shown). (B, C) Neither expression of human *Ptc-1* nor *Gli-2* is increased by Shh overexpression.

FIGURE 7

An S12 fibroblast *Gli-1*-luciferase reporter assay confirms production, processing and secretion of functional Hedgehog ligand by LNCaP cells overexpressing Shh. Comparison of the LNCaP parent cell line with the LNCaP$^{Shh(M)}$and LNCaP$^{Shh(H)}$ cell lines demonstrates robust hedgehog signaling activity by the overexpressing cell lines, comparable to that seen with other cell lines known to exert robust Shh signaling activity (unpublished observations).

FIGURE 8

Histology of xenograft tumors made with the LNCaP parent cell line (A, C) and the LNCaP$^{Shh(H)}$ overexpresser (B,D). Low power views show comparable stromal and epithelial composition in the control (A) and overexpresser (B) xenografts. High power views show similarity in tumor cell differentiation and density. Mitotic figures (arrow) are evident in both the control (C) and overexpresser (D) xenografts. Samples were paraformaldehyde-fixed, paraffin-sectioned and processed for standard eosin & hematoxylin histology. The size marker denotes 100μM.

FIGURE 9

Quantitative RT-PCR analysis of Hedgehog pathway genes in xenograft tumors. (A) *Shh* is overexpressed in LNCaP$^{Shh(H)}$ overexpresser xenograft tumors as compared to the tumors generated with the parent cell line. The level of expression in the parent LNCaP cell line is three orders of magnitude less and too low to be seen in this graph. (B) An assay for mouse *Ptc-1* expression using mouse-specific primers shows significantly increased *Ptc-1* expression in overexpresser xenograft tumors, as do assays for mouse *Gli-1* (C) and *Gli-2* (D). Of note, approximately equivalent high level mouse Ptc-1, Gli-1 and Gli-2 expression was observed in xenograft tumors made with the LNCaP$^{Shh(M)}$ and LNCaP$^{Shh(H)}$ cell lines (not shown), indicating that in the presence of high levels of Shh expression, stromal gene activation reaches a plateau which is independent of the absolute concentration of Shh protein produced by the epithelium.

FIGURE 10

Localization of mouse *Ptc-1* and *Gli-1* expression in the xenograft tumor. No detectable *Shh* signal is seen in the LNCaP parent cell line xenograft tumor. In the LNCaP$^{Shh(H)}$ xenograft strong epithelial *Shh* expression is mirrored by mouse *Ptc-1* and *Gli-1* expression in the tumor stroma. Expression of the indicated genes was investigated in paraffin sections. Due to extremely high expression levels, only brightfield images were captured for *Shh* and *actin*, in which the radioactive signal is visible as black silver grains. For Ptc-1 and Gli-1, bright-field and corresponding dark-field images were superimposed and radioactive signals filled in with artificial color (red and pink).

FIGURE 11

Shh overexpression increases xenograft tumor growth. The LNCaP, LNCaP$^{GFP}$, LNCaP$^{Shh(M)}$, and LNCaP$^{Shh(H)}$ xenograft tumors were grown for 8 weeks and tumor size serially determined after the appearance of visible tumors. The incidence of tumors generated with the various cell lines was comparable; in the few cases where a tumor did not form it was not counted in the analysis. (A) Average tumor size by line. The rates of tumor growth were determined by averaging the tumor size for mice in each cell line at each time point. Vertical bars are ±SEM. Points and lines are offset horizontally to prevent overlap. (B) Average slope for each of the individual tumor growth curves over the 3-8 week period. The mean slopes (+) for each tumor group are significantly different: LNCaP versus LNCaP$^{GFP}$ (P= 0.0047), LNCaP$^{Shh(M)}$ (P=0.0084) and LNCaP$^{Shh(H)}$ (P=0.0001); LNCaP$^{GFP}$ versus LNCaP$^{Shh(M)}$ (P=0.0001) and LNCaP$^{Shh(H)}$ (P=0.0001); and LNCaP$^{Shh(M)}$ versus LNCaP$^{Shh(H)}$ (P=0.002).

FIGURE 12

Schematic model for the action of *Shh* in prostate tumor growth. Shh expressed by tumor cells acts upon nearby stromal cells to induce the expression *Gli-1* and activate the expression of target genes which may positively regulate tumor cell proliferation either through effects on the tumor cells in a paracrine signaling loop, or through indirect effects such as stimulation of angiogenesis.

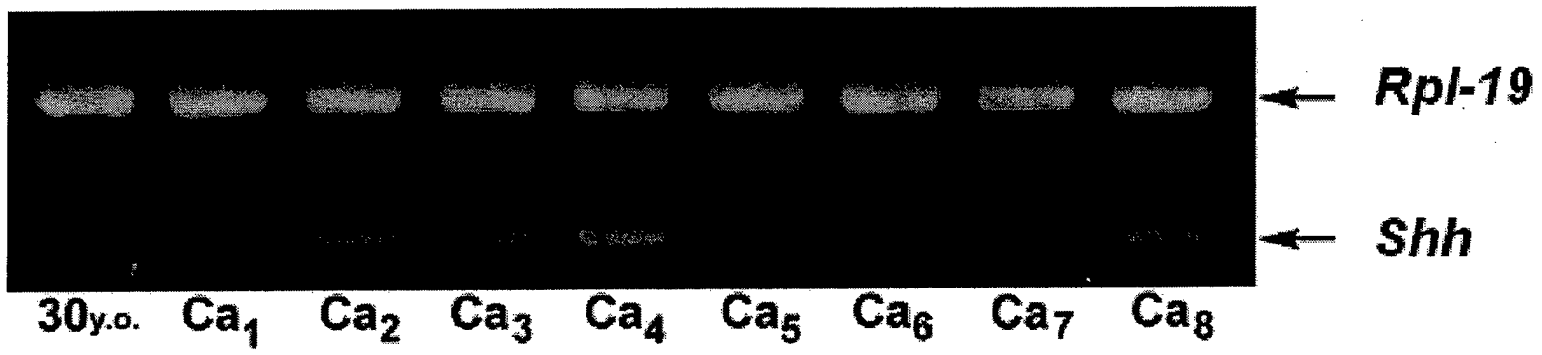
Rpl-19
Shh
30y.o.
Ca1
Ca2
Ca3
Ca4
Ca5
Ca6
Ca7
Ca8

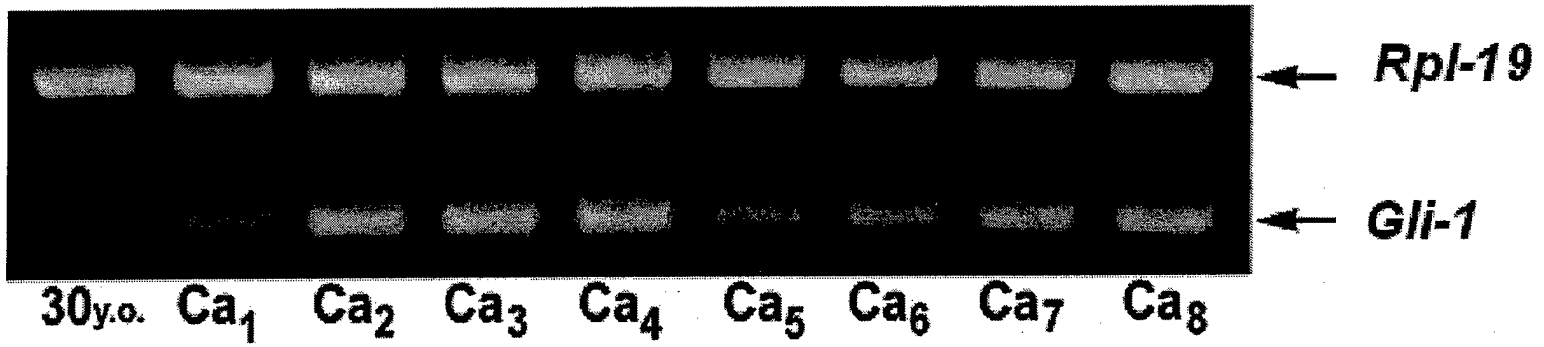
Rpl-19
Gli-1
30y.o.
Ca1
Ca2
Ca3
Ca4
Ca5
Ca6
Ca7
Ca8

Figure 1

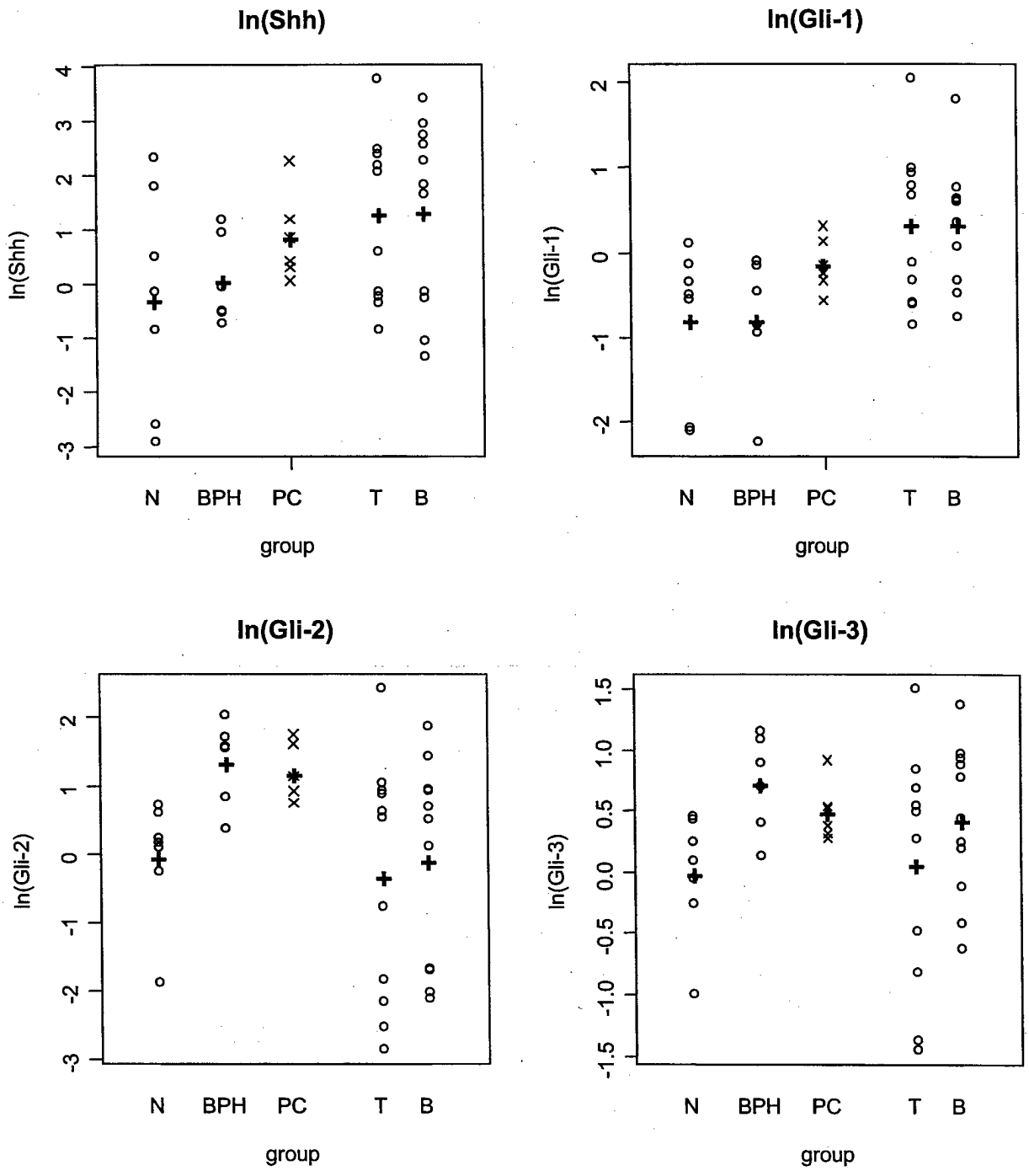
ln(Shh)
ln(Shh)
-3
-2
-1
0
1
2
3
4
N
BPH
PC
T
B
group
ln(Gli-1)
ln(Gli-1)
-2
-1
0
1
2
N
BPH
PC
T
B
group
ln(Gli-2)
ln(Gli-2)
-3
-2
-1
0
1
2
N
BPH
PC
T
B
group
ln(Gli-3)
ln(Gli-3)
-1.5
-1.0
-0.5
0.0
0.5
1.0
1.5
N
BPH
PC
T
B
group

Figure 2A

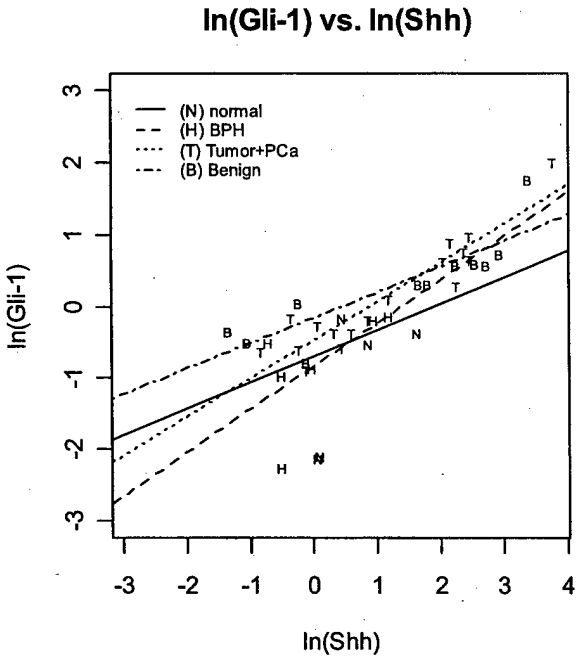
ln(Gli-1) vs. ln(Shh)
(N) normal
(H) BPH
(T) Tumor+PCa
(B) Benign
ln(Gli-1)
ln(Shh)

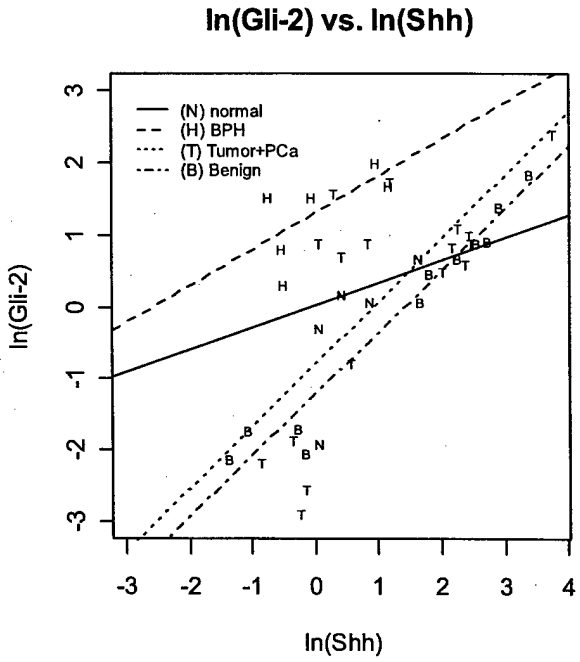
ln(Gli-2) vs. ln(Shh)
(N) normal
(H) BPH
(T) Tumor+PCa
(B) Benign
ln(Gli-2)
ln(Shh)

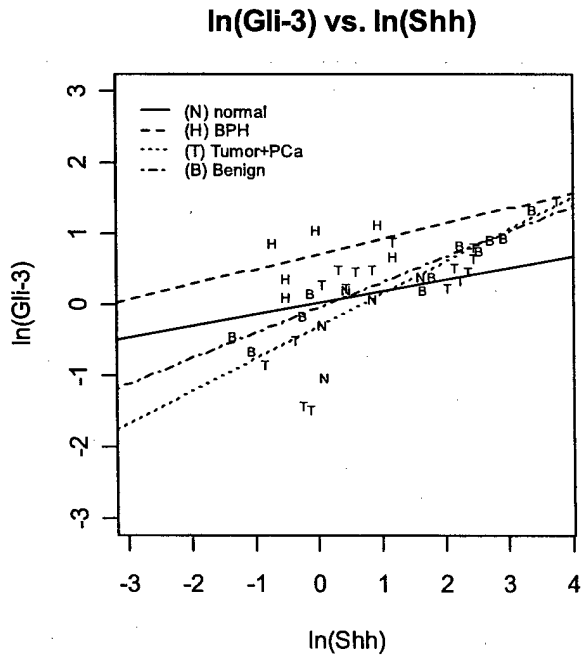
ln(Gli-3) vs. ln(Shh)
(N) normal
(H) BPH
(T) Tumor+PCa
(B) Benign
ln(Gli-3)
ln(Shh)

Figure 2B

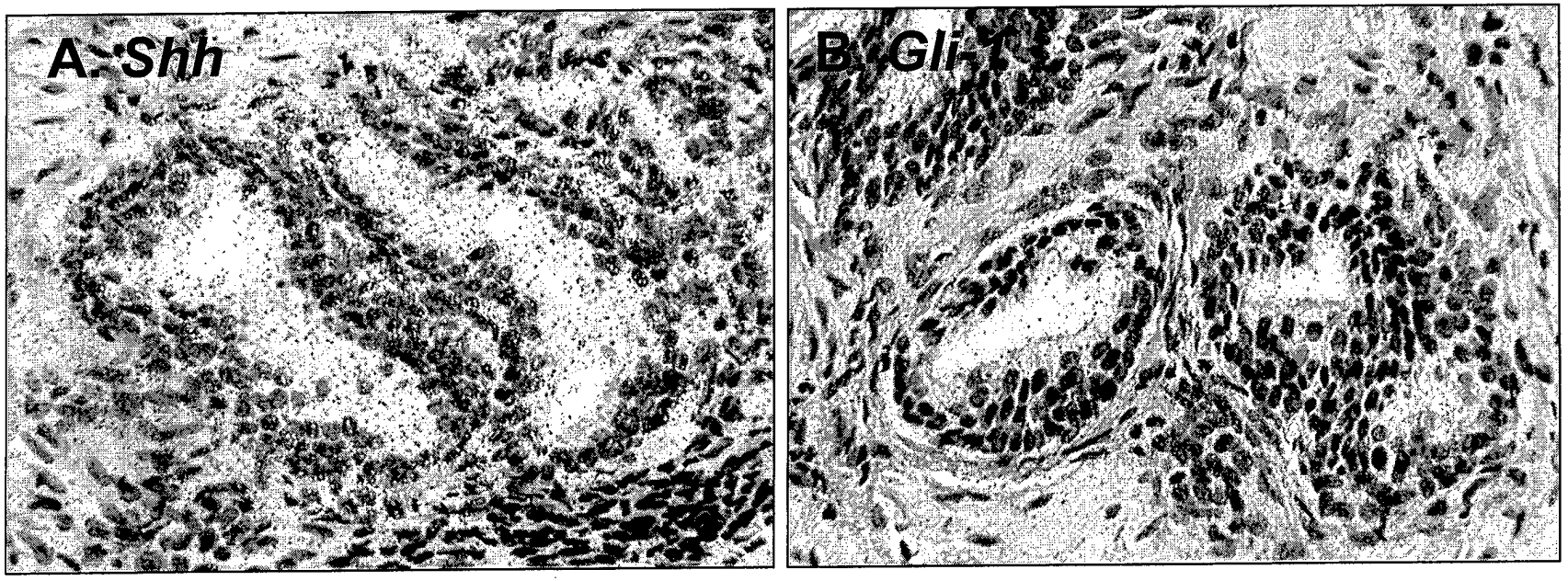


Figure 3

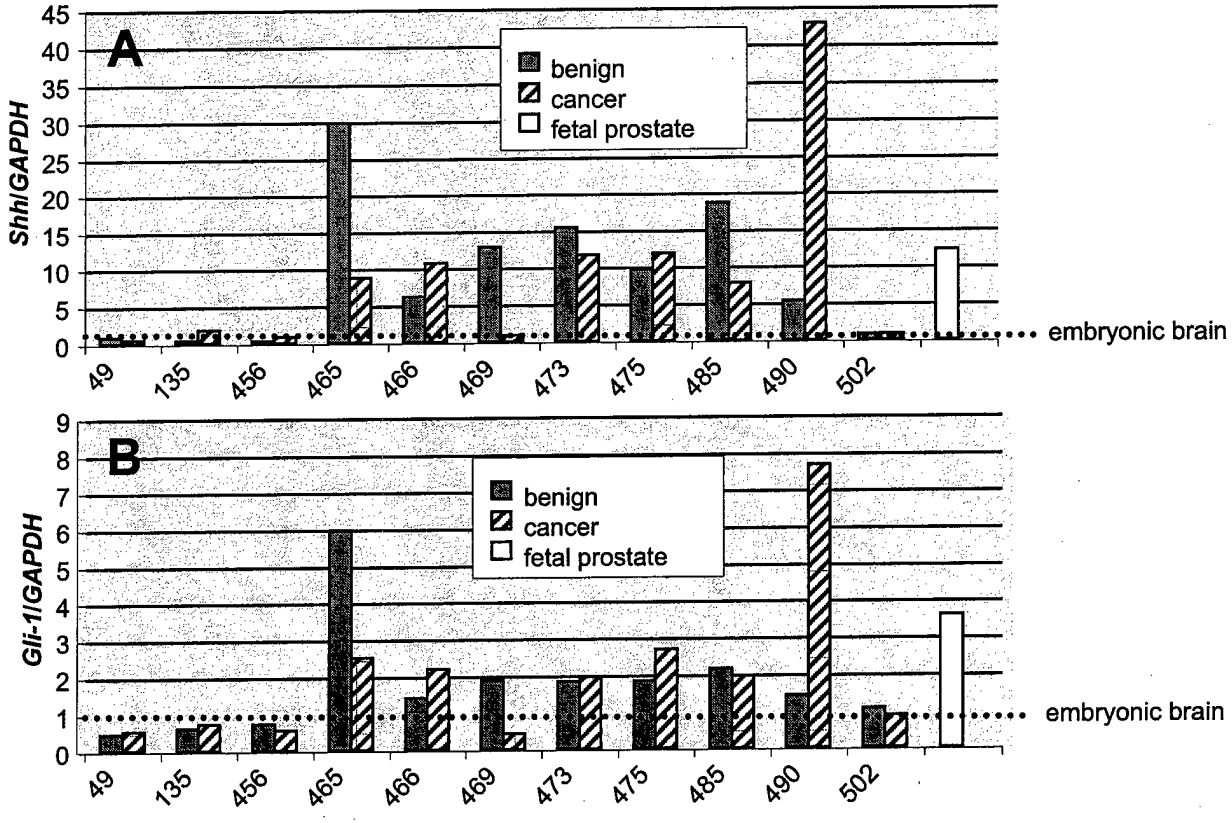
A
benign
cancer
fetal prostate
Shh/GAPDH
45
40
35
30
25
20
15
10
5
0
embryonic brain
49
135
456
465
466
469
473
475
485
490
502
B
benign
cancer
fetal prostate
Gli-1/GAPDH
9
8
7
6
5
4
3
2
1
0
embryonic brain
49
135
456
465
466
469
473
475
485
490
502

Figure 4

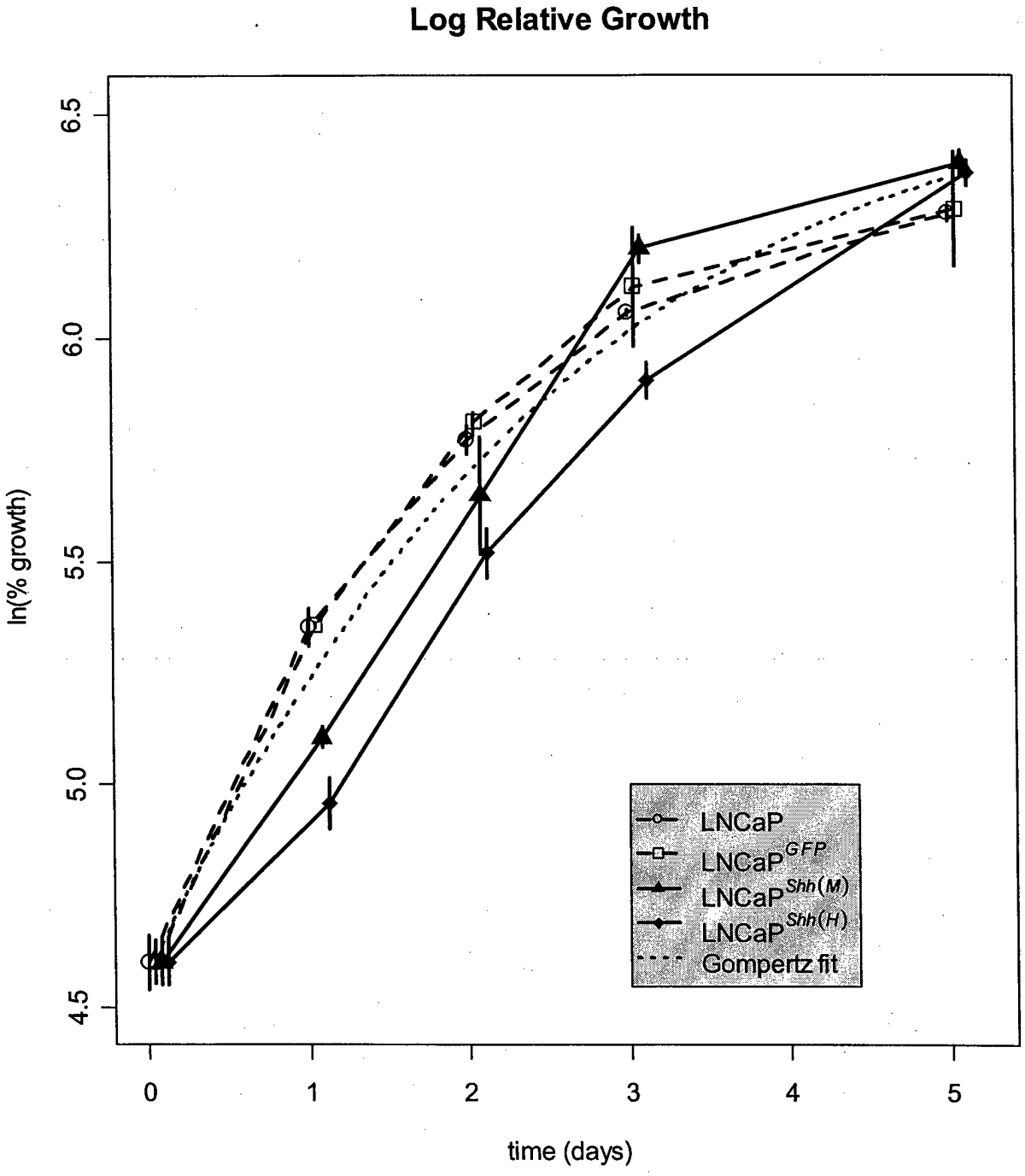
Log Relative Growth
ln(% growth)
6.5
6.0
5.5
5.0
4.5
0
1
2
3
4
5
time (days)
LNCaP
LNCaP GFP
LNCaP Shh(M)
LNCaP Shh(H)
Gompertz fit

Figure 5

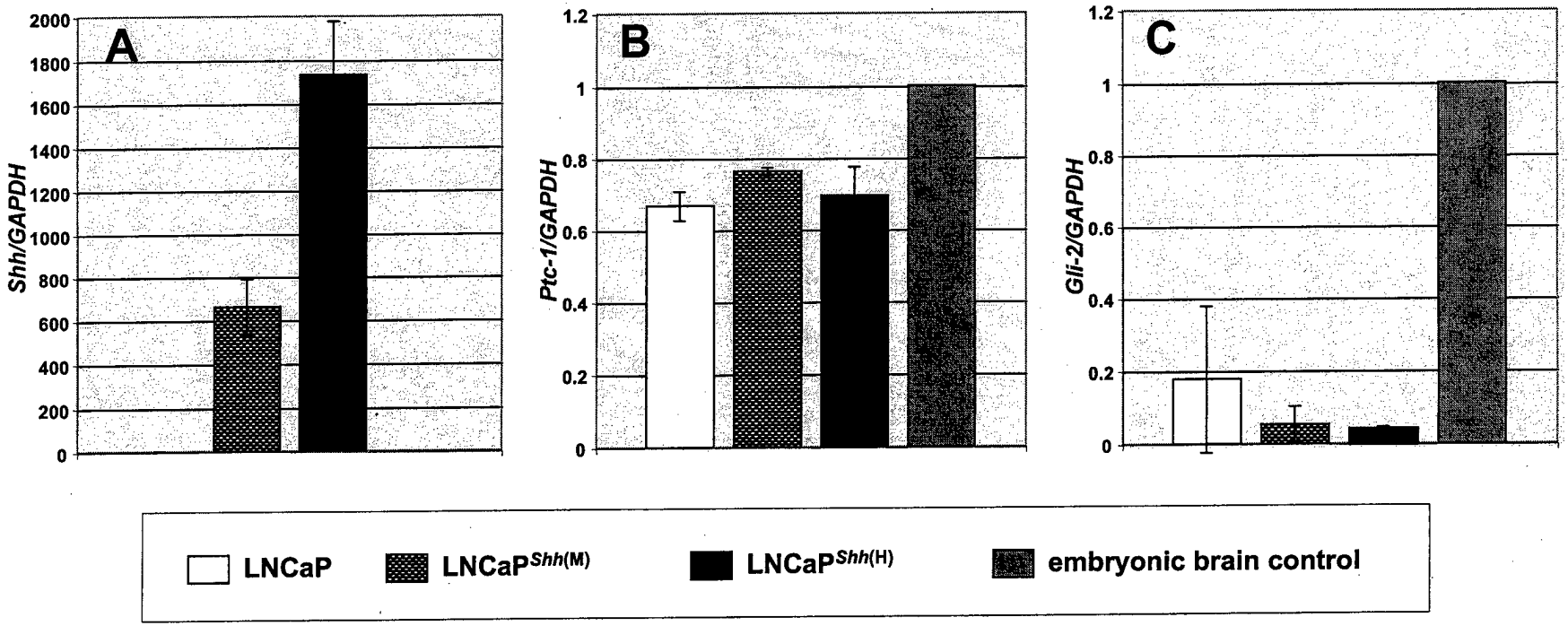


(*Gli-1* not detectable)

Figure 6

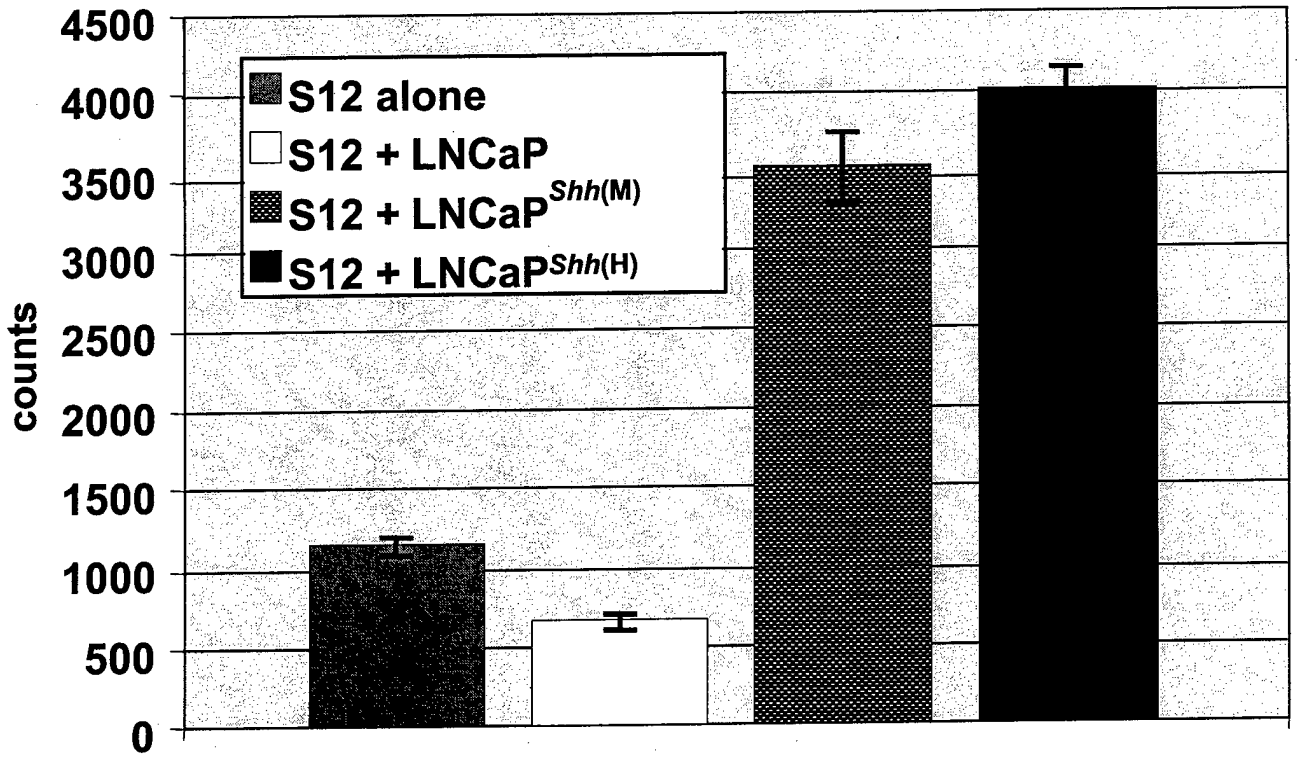
4500
4000
3500
3000
2500
2000
1500
1000
500
0
counts
S12 alone
S12 + LNCaP
S12 + LNCaP Shh(M)
S12 + LNCaP Shh(H)

Figure 7

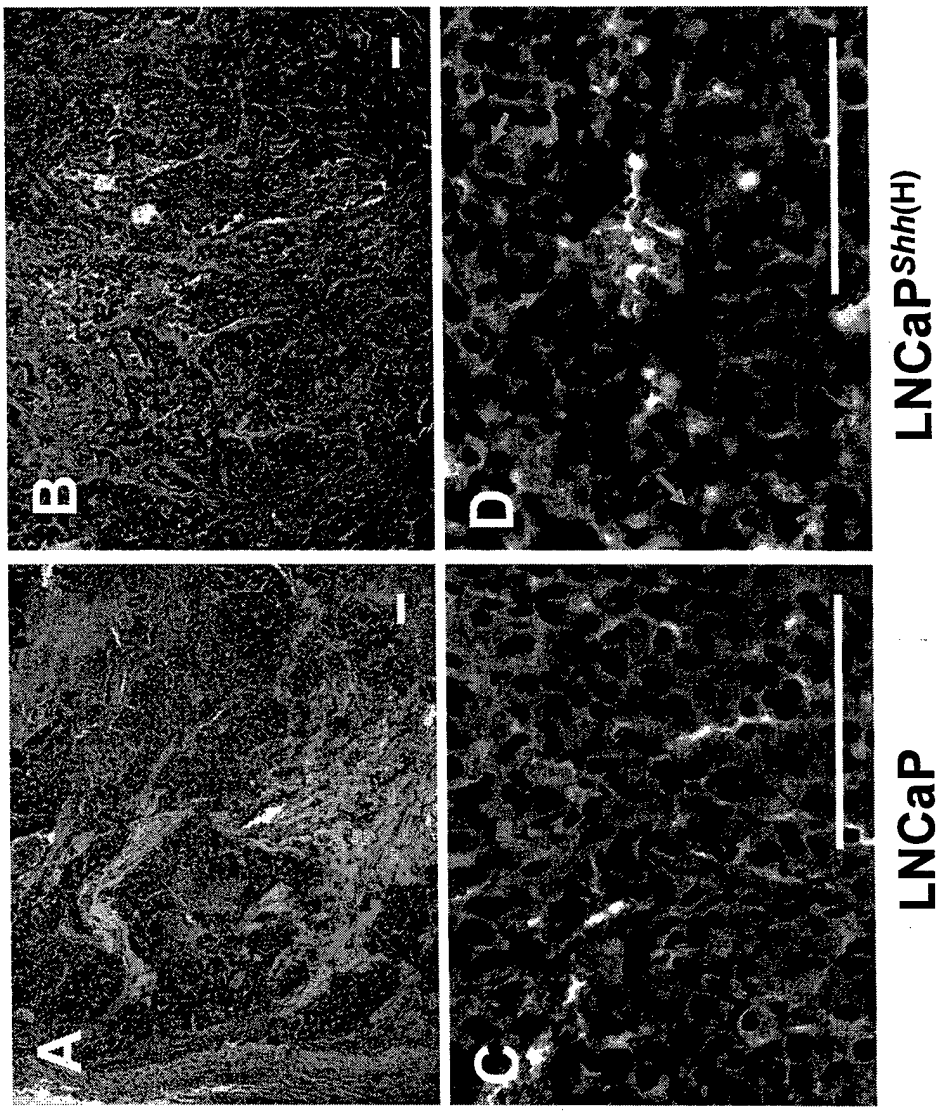


Figure 8

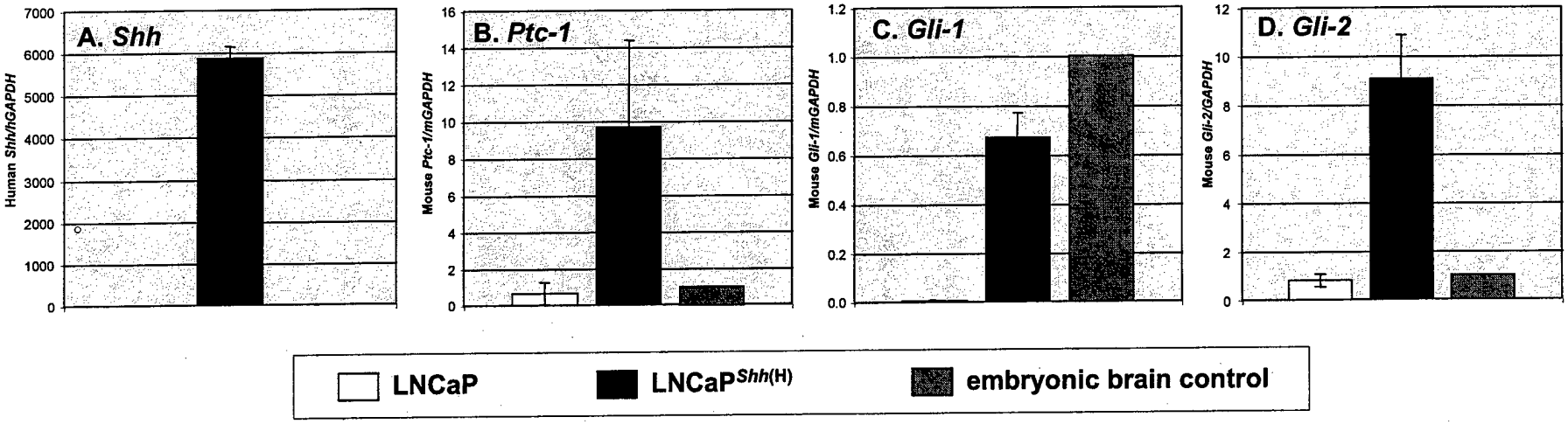
A. Shh
Human Shh/hGAPDH
7000
6000
5000
4000
3000
2000
1000
0
B. Ptc-1
Mouse Ptc-1/mGAPDH
16
14
12
10
8
6
4
2
0
C. Gli-1
Mouse Gli-1/mGAPDH
1.2
1.0
0.8
0.6
0.4
0.2
0.0
D. Gli-2
Mouse Gli-2/GAPDH
12
10
8
6
4
2
0
LNCaP
LNCaP Shh(H)
embryonic brain control

Figure 9

# Hedgehog Pathway Genes in Xenograft Tumors

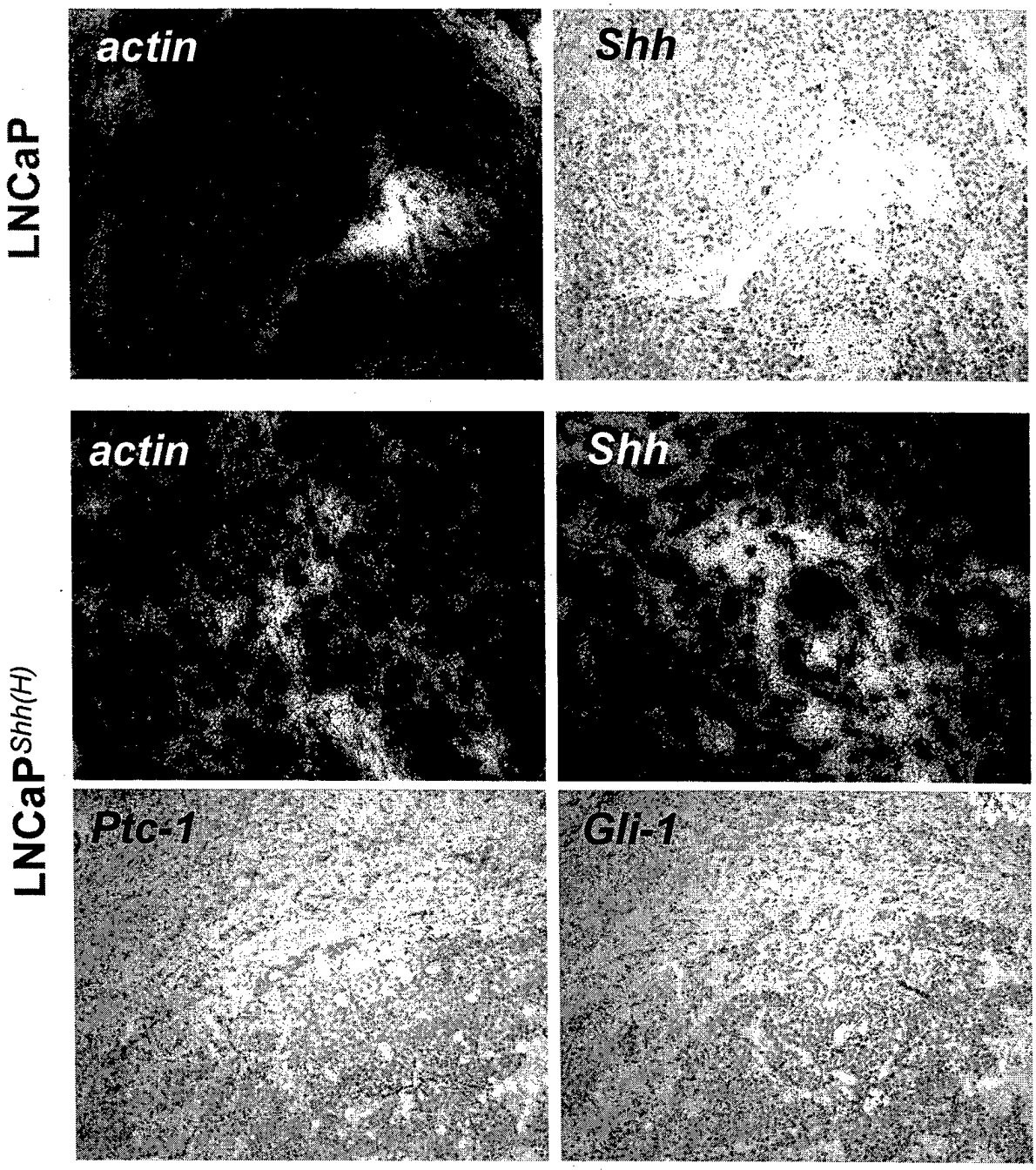


Figure 10

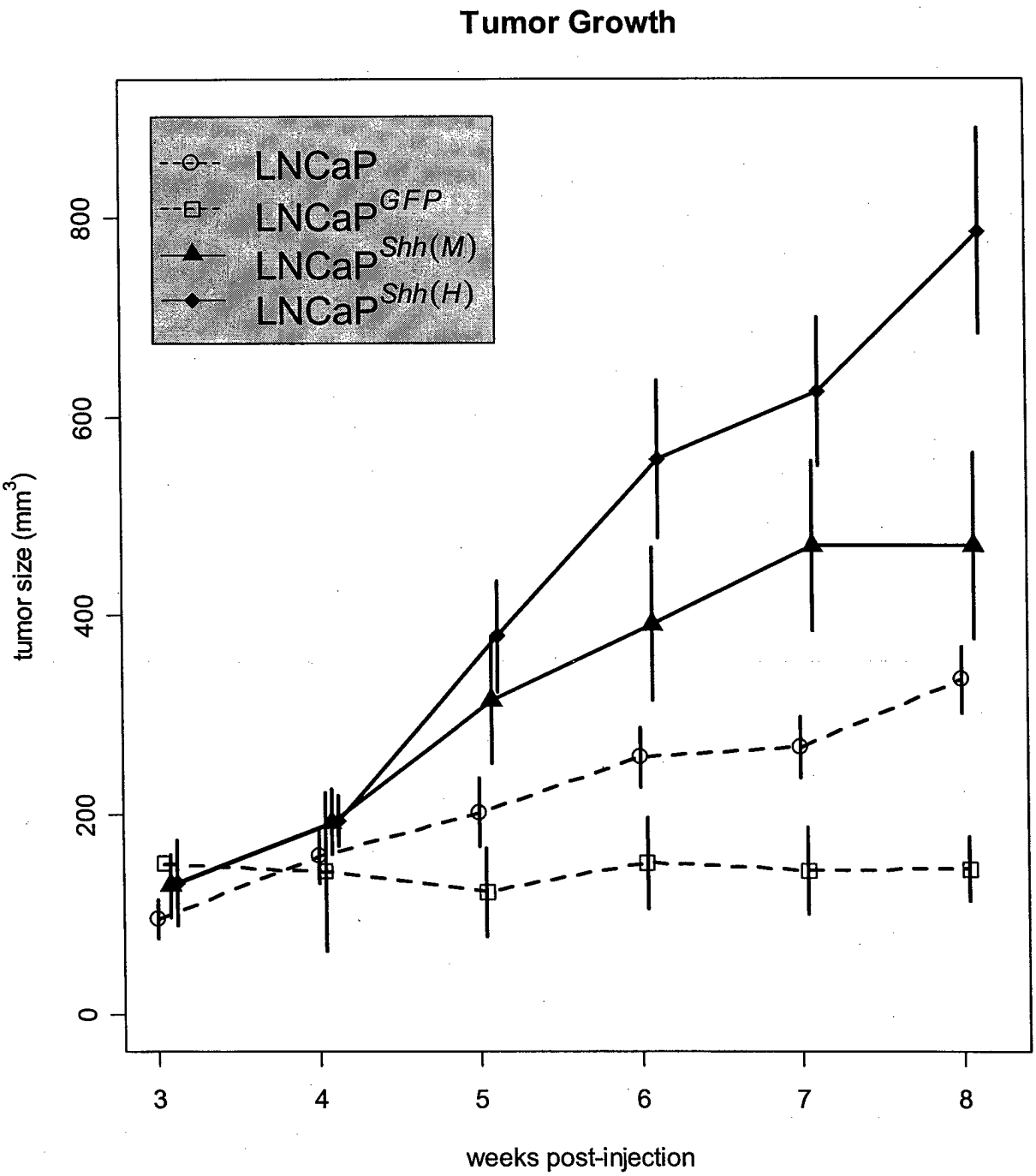
Tumor Growth
LNCaP
LNCaP GFP
LNCaP Shh(M)
LNCaP Shh(H)
tumor size (mm3)
0
200
400
600
800
3
4
5
6
7
8
weeks post-injection

Figure 11 *A*

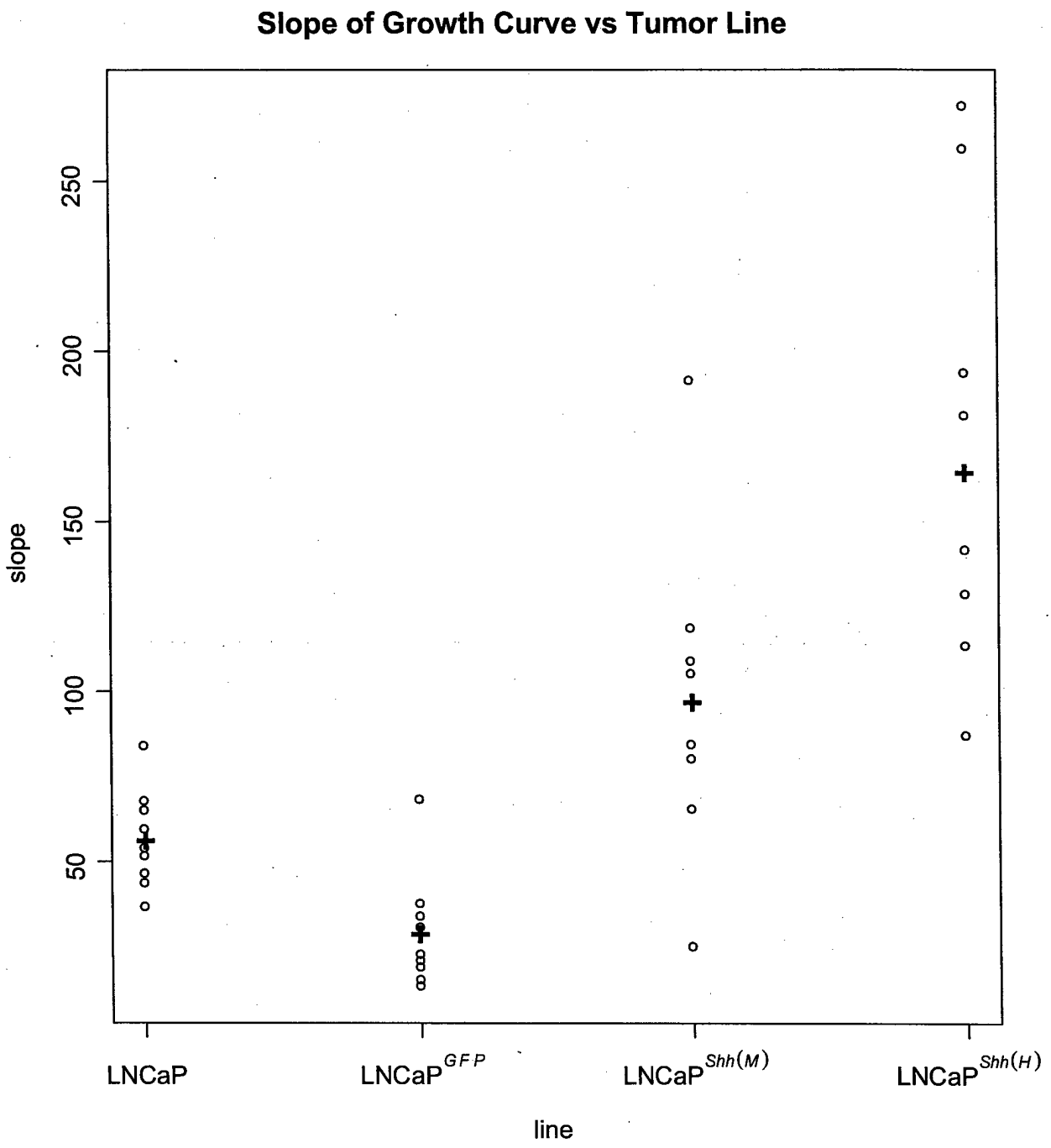
Slope of Growth Curve vs Tumor Line
slope
50
100
150
200
250
LNCaP
LNCaP^GFP
LNCaP^Shh(M)
LNCaP^Shh(H)
line

Figure 11B

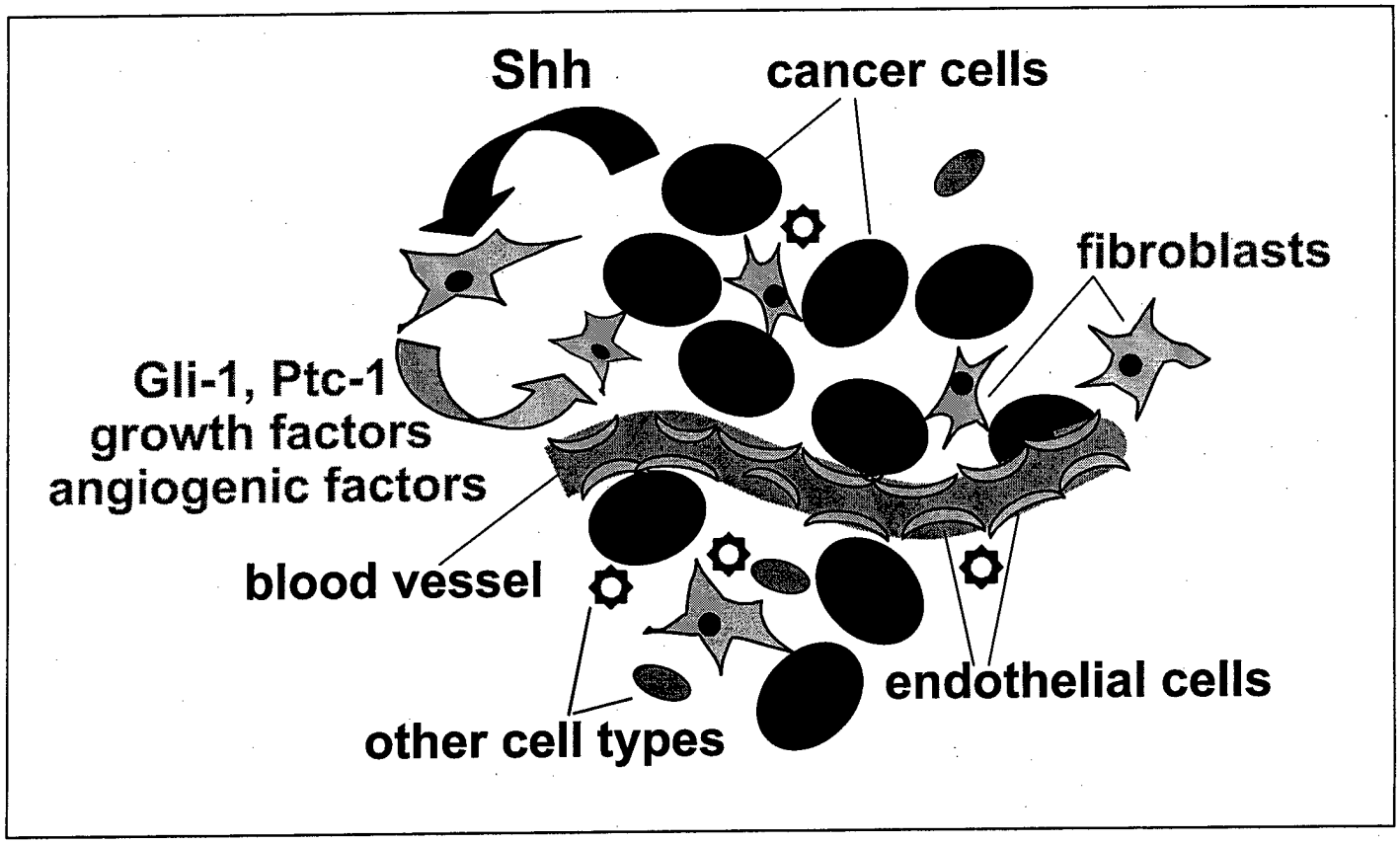
Shh
cancer cells
fibroblasts
Gli-1, Ptc-1
growth factors
angiogenic factors
blood vessel
endothelial cells
other cell types

Figure 12